

1 **HDM-Plot: a plot dataset of plant communities across three-dimensional zonal**
2 **vegetation in the Hengduan Mountains and adjacent regions, southwestern China**

3 Yili Jin, Liuyiyi Yang, Xiaofei Hu, Chen Yang, Haojun Xia, Ying Hou, Kai Wu, Shaolin Shi,
4 Xingxing Mao, Jian Ni

5 College of Life Sciences, Zhejiang Normal University, Jinhua 321004, China

6 Correspondence: Xingxing Mao (xyz1314@zjnu.edu.cn); Jian Ni (nijian@zjnu.edu.cn).

7 **Abstract.** The Hengduan Mountains (HDM) constitute one of the world's richest biodiversity
8 regions and are designated as a top-tier priority for ecological conservation. Vegetation investigation
9 can help with the design and implementation of biodiversity conservation in this region. Here we
10 present the HDM-Plot, a plot-based vegetation dataset compiled from 314 plots surveyed during
11 four campaigns between 2022 and 2024 across the Hengduan Mountains and adjacent regions,
12 across major vegetation types from lowland dry-hot valleys to alpine areas spanning altitudes of
13 754–4,932 m. Each plot records detailed species-level information, including scientific name,
14 growth form, life form, number of individuals or clumps, plant height, diameter at breast height or
15 at base, crown width, and coverage, along with geographic coordinates and hierarchical vegetation
16 classification. In total, the dataset comprises 14,113 individual records belonging to 1,127 species
17 from 379 genera and 117 families. The dominant families are Rosaceae (133 species), Ericaceae
18 (93), Fabaceae (66), Asteraceae (63), and Fagaceae (37), and the dominant genera are *Rhododendron*
19 (75), *Berberis* (34), *Cotoneaster* (30), *Salix* (24), and *Quercus* (22), with composition varying
20 among vegetation types. Growth forms are mainly composed of shrubs (46.0%), trees (27.3%), and
21 herbs (23.6%). Herbs are dominated by perennial (92.1%), shrubs are mainly deciduous broadleaf
22 (59.7%), and trees are primarily deciduous broadleaf (46.8%) and evergreen broadleaf (41.6%).
23 Species richness, growth forms, and life forms show clear elevational changes within the HDM-Plot
24 dataset. Floristically, genus-level areal-types in the HDM-Plot dataset are dominated by temperate
25 elements (54.1%), followed by tropical elements (35.4%). 314 plots can be assigned to three
26 vegetation formation groups, 18 vegetation formations, 142 alliance groups, 209 alliances, 238
27 association groups, and 299 associations. The HDM-Plot dataset provides an updated and
28 standardized baseline for quantitative analyses of mountain vegetation, biodiversity assessment, and
29 vegetation classification and mapping in southwestern China. Such information can be future used

30 in the revisions of China's vegetation classification scheme and *Vegegraphy of China*. The dataset
31 is available from Figshare (Jin et al., 2026a; <https://doi.org/10.6084/m9.figshare.32706207>) and
32 through the National Tibetan Plateau / Third Pole Environment Data Center (Jin et al., 2026b;
33 <https://doi.org/10.11888/Terre.tpdc.303394>).

34 **1 Introduction**

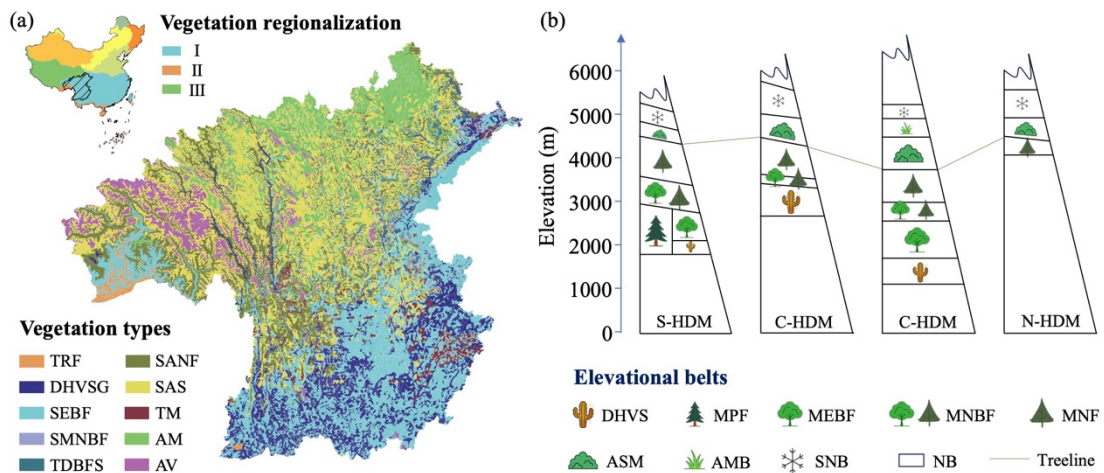
35 The Hengduan Mountains (HDM) form the core mountainous region in
36 southwestern China and are recognized as one of the world's richest biodiversity
37 hotspots and a global priority area for ecological conservation (Myers et al., 2000; Sloan
38 et al., 2014). Located at the junction between the Tibetan Plateau and the Yangtze Block,
39 the HDM represents a young and rapidly evolving orogenic belt shaped by ongoing
40 tectonic uplift associated with Indian–Eurasian collision (Xing and Ree, 2017). Long-
41 term mountain uplift, together with intense river incision, has generated exceptional
42 topographic complexity, characterized by closely spaced north–south–oriented high
43 mountains and deeply incised valleys (Integrated Scientific Expedition to Qinghai-
44 Tibet Plateau, Chinese Academy of Sciences, 1997). As an ecotonal region linking
45 subtropical lowlands to alpine highlands, the HDM is affected by the southwest and
46 southeast monsoons as well as mesoscale atmospheric systems (Wu et al., 2012; Zhang
47 et al., 2024). These interacting geological and climatic processes create strong
48 environmental heterogeneity, supporting abundant biodiversity, significant spatial
49 differentiation of ecosystems, and complex vegetation distribution (Liang et al., 2018;
50 Ding et al., 2020; He et al., 2020). Consequently, robust characterization of species
51 composition, community structure, and vegetation zonation in the HDM is essential for
52 biodiversity conservation and sustainable development, thereby provides key empirical
53 support for advancing studies of global mountain biogeography and ecology.

54 Vegetation represents the most visible and distinctive ecological feature of a region,
55 and plot-based plant community data provide the fundamental basis for documenting
56 vegetation composition and distribution patterns, as well as for the compilation of the
57 *Vegegraphy*—a series of monographs that describe detailed species composition,

58 structures, functions, environmental settings, and distribution of a set of plant
59 communities and/or their combinations for each vegetation type, using community data
60 from vegetation survey (Fang et al., 2020; Wang et al., 2020; Sabatini et al., 2021). Over
61 recent decades, extensive vegetation surveys have been conducted across the HDM and
62 its adjacent mountains and plateaus, including those in the First (1970–1990) and
63 Second (2018–2024) Tibetan Plateau Scientific Expeditions, and numerous regional
64 surveys (the late 20th to the early 21st Century). These efforts have substantially
65 advanced theoretical knowledge of floristic composition (Li, 1988; Shen et al., 2004;
66 Xu et al., 2014; Yu et al., 2020), community structure (Sherman et al., 2008; Xu et al.,
67 2008; Sun et al., 2017), vegetation distribution (Yao et al., 2010; Liang et al., 2018; Wu
68 and Yu, 2020; Zhang et al., 2023), eco-geographical regionalization (Zheng and Yang,
69 1987; Yang and Zheng, 1989; Chi et al., 2019), and vegetation modeling (He et al., 2020;
70 Yin et al., 2020), with sustained attention to dry-hot valley vegetation (Jin and Ou, 2000;
71 Jin, 2002; Liu et al., 2016a, b; Yang J D et al., 2016; Yang Y et al., 2016).

72 Existing plot surveys consistently indicate significant horizontal differentiation
73 and elevational turnover in HDM vegetation (Editorial Committee of Vegetation Map
74 of China, the Chinese Academy of Sciences, 2007a, b). In the vegetation regionalization
75 scheme of China, the study region spans three vegetation regionalization units: the
76 subtropical evergreen broadleaf forest region, the Qinghai-Xizang Plateau alpine
77 vegetation region, and the tropical monsoon rain forest and rain forest region (Fig. 1a;
78 Table S1; Editorial Committee of Vegetation Map of China, the Chinese Academy of
79 Sciences, 2007b). Across the region, from the southeast toward the northwest,
80 vegetation types shift from subtropical evergreen broadleaf forests and dry-hot valley
81 shrubby grasslands to subalpine needleleaf forests, subalpine shrublands, and alpine
82 meadows (Fig. 1a; Table S1; Editorial Committee of Vegetation Map of China, the
83 Chinese Academy of Sciences, 2007a). Along elevational gradients, vegetation belt
84 spectra typically transition from the dry-hot valley shrubland belt through the belts of
85 mountains evergreen broadleaf forest, mixed needleleaf and broadleaf forest, and
86 needleleaf forest, to the belts of alpine shrubland and meadow, alpine meadow, and the
87 nival (Fig. 1b; Zheng, 1988). Despite a large number of community plot data

88 accumulated by earlier surveys, many datasets remain difficult to integrate for synthesis
 89 due to extended temporal spans, limited accessibility of original records, heterogeneous
 90 study designs, as well as inconsistent taxonomic and classification frameworks across
 91 campaigns. Meanwhile, vegetation on the Tibetan Plateau including the HDM has been
 92 reshaped under increasing climate change and human activities (Zhang et al., 2015;
 93 Piao et al., 2019), highlighting the need for updated, standardized, and openly available
 94 plot-based plant community data.



95
 96 **Figure 1.** Horizontal (a) and elevational (b) patterns of vegetation distribution in the Hengduan
 97 Mountains (HDM) and adjacent regions—the HDM-Plot study region. Vegetation regionalization
 98 was obtained from the *Vegetation Regionalization Map of China* (Editorial Committee of Vegetation
 99 Map of China, the Chinese Academy of Sciences, 2007b). I, subtropical evergreen broadleaf forest
 100 region; II, tropical monsoon rain forest and rain forest region; and III, Qinghai-Xizang Plateau alpine
 101 vegetation region. Vegetation types were extracted from the *1:1,000,000 Vegetation Map of the
 102 People's Republic of China* (Editorial Committee of Vegetation Map of China, the Chinese Academy
 103 of Sciences, 2007a). The original 35 vegetation formations were aggregated into 10 categories based
 104 on climatic zone, community structure, and ecological function. TRF, tropical rain forest; DHVSG,
 105 dry-hot valley shrubby grassland; SEBF, subtropical evergreen broadleaf forest; SMNBF,
 106 subtropical mountains mixed needleleaf and broadleaf forest; TDBFS, temperate deciduous
 107 broadleaf forest and shrubland; SANF, subalpine needleleaf forest; SAS, subalpine shrubland; TM,
 108 temperate meadow; AM, alpine meadow; and AV, alpine cushion and sparse vegetation, and bare
 109 land. Elevational vegetation belt spectra for the southern (S-HDM), central (C-HDM), and northern
 110 (N-HDM) sectors of the Hengduan Mountains were revised after Zheng (1988). DHVS, dry-hot
 111 valley shrubland belt; MPF, mountains *Pinus* forest belt; MEBF, mountains evergreen broadleaf
 112 forest belt; MNBF, mountains mixed needleleaf and broadleaf forest belt; MNF, mountains
 113 needleleaf forest belt; ASM, alpine shrubland and meadow belt; AMB, alpine meadow belt; SNB,
 114 subnival belt; and NB, nival belt.

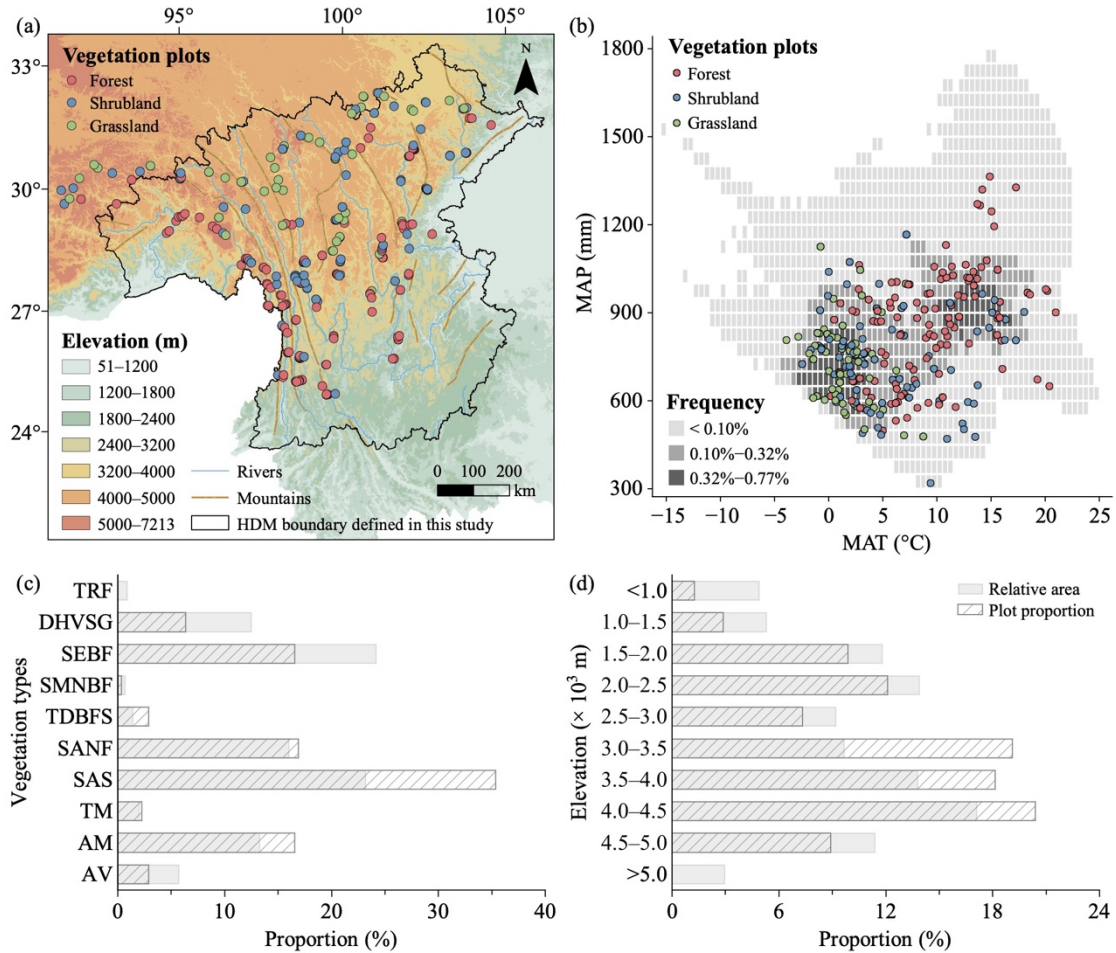
115 To provide an up-to-date baseline of vegetation composition and spatial patterns

116 in the HDM and adjacent regions, we conducted four large-scale surveys between 2022
117 and 2024 along the major mountains and valleys, spanning tropical, subtropical, and
118 temperate zones and extending into subalpine and alpine environments, in accordance
119 with the horizontal and vertical zonation. We surveyed 314 plant community plots and
120 integrated all field records into a standardized plot-based vegetation dataset, HDM-Plot.
121 It documents plant species composition and taxonomic attributes and supports a
122 consistent vegetation classification across the region. The HDM-Plot dataset provides
123 a contemporary and standardized baseline for plant community study and long-term
124 monitoring of vegetation, and serves as a vital reference for biodiversity conservation,
125 vegetation restoration, and sustainable development. It also offers empirical support for
126 revising of the China's vegetation classification scheme (Guo et al., 2020) and the
127 compilation of the *Vegegraphy of China* (Fang et al., 2020).

128 **2 Study area**

129 The HDM covers a broad geographical extent, and their spatial boundaries can
130 vary slightly among studies depending on research objectives. In this study, we use the
131 HDM boundary (24.08°–34.32° N, 93.13°–106.16° E, 119–7,213 m; Fig. 2a) following
132 Yu et al. (1989) and Zhang et al. (1997) as the geographical core of the study region.
133 Because of the continuity of regional topography, the gradual transition of vegetation
134 belts, and the practical arrangement of survey routes, the actual survey extent included
135 adjacent regions along the southeastern and northwestern margins (Fig. 2a). These
136 peripheral plots record important vegetation transitions from the HDM toward adjacent
137 regions, and were therefore retained. Unless otherwise specified, the “HDM-Plot study
138 region” in this manuscript refers to the HDM and adjacent regions covered by our field
139 surveys, rather than to the HDM *sensu stricto*. The region exhibits an overall increase
140 in elevation from the southeast toward the northwest and is characterized by a series of
141 north–south–oriented mountains and deeply incised valleys. Climatically, the HDM-
142 Plot study region spans tropical, subtropical, temperate, and alpine zones, with mean
143 annual temperature ranging from –18.2 to 25.1 °C. Warmer conditions are concentrated

144 in the dry-hot valleys and lower subtropical mountains in the southeast, and in the
 145 tropical rainforests along the western margin, while much lower temperatures occur
 146 across the highlands toward the northwest. Mean annual precipitation across the region
 147 varies but is generally lower (0–1,793 mm), and relatively humid conditions are mainly
 148 associated with the southwestern and southeastern margins (Fig. 2b).



149 **Figure 2.** Spatial (a), climatic (b), vegetation-type (c), and elevational (d) coverage of vegetation
 150 plots in the HDM-Plot dataset. Elevation data (m) were derived from the SRTM 90 m dataset (Farr
 151 et al., 2007) and resampled into 1 km grid cells. Mountain and river data were obtained from the
 152 Digital Mountain Map of China Dataset (Nan et al., 2015) and Natural Earth
 153 (<https://www.naturalearthdata.com>, last access: 12 March 2026), respectively. Mean annual
 154 temperature (MAT, °C) and mean annual precipitation (MAP, mm) were derived from a 1 km
 155 monthly climate dataset for China covering 1991–2020 (Hu et al., 2025). Grey cells in panel (b)
 156 indicate the frequency of MAT–MAP combinations among all 1 km grid cells within the study
 157 boundary, based on two-dimensional bins of 0.5 °C for MAT and 50 mm for MAP. In panels (c) and
 158 (d), grey bars indicate the relative area of each vegetation type and elevational belt within the study
 159 region, and hatched bars represent the proportion of surveyed plots within each group. Vegetation
 160 types were extracted from the *1:1,000,000 Vegetation Map of the People’s Republic of China*
 161 (Editorial Committee of Vegetation Map of China, the Chinese Academy of Sciences, 2007a). TRF,
 162 tropical rain forest; DHVSG, dry-hot valley shrubby grassland; SEBF, subtropical evergreen
 163

164 broadleaf forest; SMNBF, subtropical mountain mixed needleleaf and broadleaf forest; TDBFS,
165 temperate deciduous broadleaf forest and shrubland; SANF, subalpine needleleaf forest; SAS,
166 subalpine shrubland; TM, temperate meadow; AM, alpine meadow; and AV, alpine cushion
167 vegetation, alpine sparse vegetation, and bare land.

168 **3 Materials and Methods**

169 **3.1 Vegetation survey**

170 Field surveys were conducted during four campaigns in March 2022, May–June
171 2022, May–June 2023, and June 2024. May–June was selected as the primary survey
172 time because most species across elevational belts in the region have developed
173 diagnostic vegetative structures and even many have begun flowering, enabling reliable
174 identification. In addition, it coincides with the transition from the dry to the wet season
175 when precipitation is still relatively low and field accessibility is generally high. An
176 additional survey in March 2022 targeted dry-hot valley vegetation, where phenological
177 development occurs earlier under warm and relatively arid conditions.

178 To capture the major vegetation belts and transition zones shaped by the regional
179 mountain–valley and climatic gradients, we adopted a coverage-oriented field sampling
180 design. Plots were set up across representative mountains and valleys of the HDM and
181 adjacent regions along various longitudinal, latitudinal, and elevational gradients. The
182 survey aimed to cover major vegetation physiognomic types, representative mountain–
183 valley systems, and local transitions among forest, shrubland, and grassland
184 communities. Field logistics, road accessibility, and terrain conditions were also
185 considered during plot selection. Plot size was determined following community
186 physiognomy and stand heterogeneity. The sizes of grassland plots were mainly 1 m ×
187 1 m (91.9% of grassland plots), of shrubland plots were mainly 5 m × 5 m (70.0%), and
188 of forest plots were mainly 10 m × 10 m (56.3%) or 10 m × 20 m (29.6%). Local
189 adjustments in plot size were made because of terrain constraints, especially slope, and
190 field operability in complex mountain environments. The dominant plot size covered
191 broad spatial and elevational ranges within the surveyed distribution of their
192 corresponding vegetation types (Fig. S1; Table S2). In forest and shrubland plots, all

193 woody species were recorded, including species name, growth form, phenological
194 period, number of individuals or clumps, height, stem diameter, and crown width.
195 Diameter was generally measured as diameter at breast height (DBH). For individuals
196 < 2 m tall or when DBH was not applicable, basal diameter (BD) was recorded. In forest
197 plots, individuals with height ≥ 5 m were assigned to the tree layer, whereas shrubs and
198 tree seedlings with height < 5 m were classified into the shrub layer. In grassland plots,
199 all herbaceous species were recorded, including species name, growth form,
200 phenological period, number of individuals or clumps, maximum leaf-layer height, and
201 coverage. The number of individuals or clumps was used as the count-based abundance
202 measure. For species occurring as discrete individuals, each individual was counted
203 separately. For clumped plants, distinguishable clumps were used as the counting unit,
204 and the number of individuals within clumps was additionally noted when identifiable.
205 In forest and shrubland plots, woody plants were recorded by individual or clump;
206 therefore, the same species could have multiple records within a plot. In grassland plots,
207 herbaceous plants were recorded by species, with each species represented by one
208 record containing the total number of individuals or clumps within the plot.

209 For each plot, longitude, latitude, elevation, community height and total coverage,
210 as well as disturbance intensity were recorded. The global position system was used to
211 determine the geographic coordinates. Community height was defined as the maximum
212 height of the dominant vegetation layer within a plot. Specifically, in forest plots, it
213 referred to the visually estimated height of the tallest tree in the tree layer; in shrubland
214 plots, it was measured or estimated as the height of the tallest shrub layer using a tape
215 measure where possible; and in grassland plots, it was measured as the maximum height
216 of the herbaceous leaf layer. Total coverage was visually estimated as the vertically
217 projected percentage cover of all plant species within each plot. Disturbance intensity
218 was assessed directly at four levels: none, weak, medium, and strong. These
219 measurements and estimates followed the same field criteria throughout all survey
220 campaigns and were conducted by experienced vegetation investigators to ensure
221 consistency. In total, 314 plots were surveyed, belonging to 142 forest plots, 110
222 shrubland plots, and 62 grassland plots (Fig. 2; Table 1). These surveyed plots cover the

223 major geographical space (Fig. 2a), climatic space (Fig. 2b), vegetation types (Fig. 2c),
 224 and elevational belts (Fig. 2d) of the study region.

225 **Table 1** Summary statistics of plots in the HDM-Plot dataset

Plot	All	Forest	Shrubland	Grassland
Number of plots	314	142	110	62
Longitude (°E)	92.055–104.581	92.661–104.581	92.055–103.941	92.325–103.771
Latitude (°N)	25.547–33.077	25.547–32.749	25.557–33.065	26.423–33.077
Elevation (m)	754–4932	754–4377	1144–4758	3168–4932
SR (species / plot)	1–37 (11 ± 6)	2–37 (13 ± 7)	1–22 (6 ± 4)	3–24 (12 ± 5)
Height (m)	0.001–49.0 (8.238 ± 8.982)	5.2–49.0 (16.0 ± 7.8)	0.1–10.0 (2.8 ± 2.2)	0.001–0.500 (0.081 ± 0.079)
Coverage (%)	10–100 (71 ± 18)	35–100 (71 ± 15)	10–100 (66 ± 20)	15–100 (79 ± 18)
Number of families	117	91	53	38
Number of genera	379	239	124	114
Number of species	1127	737	321	266

226 Values for species richness (SR), community height, and coverage are presented as ranges, with
 227 mean ± SD in parentheses.

228 3.2 Data processing and analysis

229 Species were identified following national and regional floras, including the *Flora*
 230 *Republicae Popularis Sinicae* (Editorial Committee of Flora of China, Chinese
 231 Academy of Sciences, 1959–2004), *Flora of Yunnan* (Kunming Institute of Botany,
 232 Chinese Academy of Sciences, 1977–2006), *Flora Xizangica* (Integrated Scientific
 233 Expedition to Qinghai-Tibet Plateau, Chinese Academy of Sciences, 1983–1987), and
 234 *Flora of Sichuan* (Gao et al., 1981). Final species names were then standardized and
 235 validated against the iPlant online taxonomic system (<http://www.iplant.cn/>, last access:
 236 16 January 2026). In the most recent taxonomy system of *Flora of Pan-Himalaya*
 237 (Zhang, 2010), *Kobresia* is classified into *Carex*. Given the ecological importance of

238 *Kobresia* in alpine zonal vegetation, and in order to maintain consistency with
239 vegetation literatures, we retained *Kobresia* as a traditional genus name for data
240 analyses, while the dataset provides both names.

241 Growth forms were classified from field observations following the definitions in
242 *Vegetation of China* (Editorial Committee of the Vegetation of China, 1980) into tree,
243 shrub, climber, semi-shrub, and herb. Some taxa (e.g., *Quercus* and *Rhododendron*) can
244 show both shrubs and small trees, and they were recorded at the plot level according to
245 the observed status. For regional summary analyses, each species was additionally
246 assigned a single predominant growth form based on its most frequent form seen in the
247 field across the dataset. Woody species were further divided by leaf type (needleleaf vs.
248 broadleaf) and phenology (evergreen vs. deciduous). Herbaceous species were
249 categorized into annual, biennial, and perennial life forms. Floristic areal-types of plant
250 families and genera were assigned primarily based on the *Areal-types of the World*
251 *Families* and *Chinese Genera of Seed Plants* (Wu et al., 1991, 2003), supplemented by
252 the *Floristic Statistics and Analyses of Seed Plant from China* (Li, 1996) and *Dictionary*
253 *of the Families and Genera of Chinese Vascular Plants* (iFlora Initiative of Kunming
254 Institute of Botany, Chinese Academy of Sciences, 2018).

255 Vegetation classification followed the *revised scheme of vegetation classification*
256 *system of China* (Guo et al., 2020), which adopted a three-level hierarchy (vegetation
257 formation, alliance, and association) and emphasizes constructive and dominant species
258 in reflecting the primary structural characteristics of plant communities. For each level,
259 a corresponding supplementary classification unit was defined (vegetation formation
260 group, alliance group, and association group). Dominance was identified using species
261 importance value (IV, %) calculated following Fang et al. (2009): for tree-layer species,
262 IV combined relative abundance, relative height, and relative basal area; for shrub-layer
263 species, IV combined relative abundance and relative height; and for herb-layer species,
264 relative abundance and relative coverage. Relative abundance was calculated from the
265 number of individuals or clumps, and all relative metrics were expressed as percentages
266 of the corresponding plot total. A community was assigned a single dominant species
267 when one species had $IV > 75\%$. When multiple species showed IV between 10% and

268 75%, species were designated as dominant and sub-dominant in descending order of IV
269 if interspecific IV differences exceeded 10%, and as co-dominant when IV differences
270 were $\leq 10\%$. When all species had IV $< 10\%$, the community was treated as lacking a
271 clear dominant species, and thereby species were simply ranked by IV (Wang et al.,
272 2020). Vegetation formation groups were defined by community ecological
273 physiognomy (e.g., forests), and vegetation formations by the life form of the
274 constructive species (e.g., evergreen needleleaf forests). Alliance groups were divided
275 by the genus of constructive species (e.g., *Abies* forest alliance group), and alliances by
276 the constructive species (e.g., *A. georgei* forest alliance). Association groups were
277 identified by the constructive species together with the life form of sub-dominant
278 species (e.g., *A. georgei* - shrub forest association group), and associations were
279 determined by the constructive species and sub-dominant species (*A. georgei* - *Rubus*
280 *amabilis* forest association). In the naming convention, a “-” was used to connect
281 species from different layers, and “+” was to connect multiple species within the same
282 layer (Guo et al., 2020). In addition, two-way indicator species analysis (TWINSPAN)
283 was further used as a complementary numerical classification of the vegetation plots. It
284 is a divisive hierarchical classification method that progressively partitions plots
285 according to differences in species composition and identifies indicator or diagnostic
286 species associated with each split.

287 **4 Data description**

288 **4.1 Species composition**

289 The HDM-Plot dataset compiles 14,113 individual records from 314 plots,
290 documenting 1,127 plant species (including subspecies and varieties) belonging to 379
291 genera and 117 families (Table 1). The most species-rich families are Rosaceae (133
292 species), Ericaceae (93), Fabaceae (66), Asteraceae (63), and Fagaceae (37), occurring
293 in 27.1% to 71.3% of plots (Fig. 3a; Table 2). Rosaceae is the most widely distributed
294 family in the dataset, while Fabaceae is also broadly recorded but with a relatively lower
295 plot frequency. Ericaceae and Fagaceae are mainly concentrated in the southern to

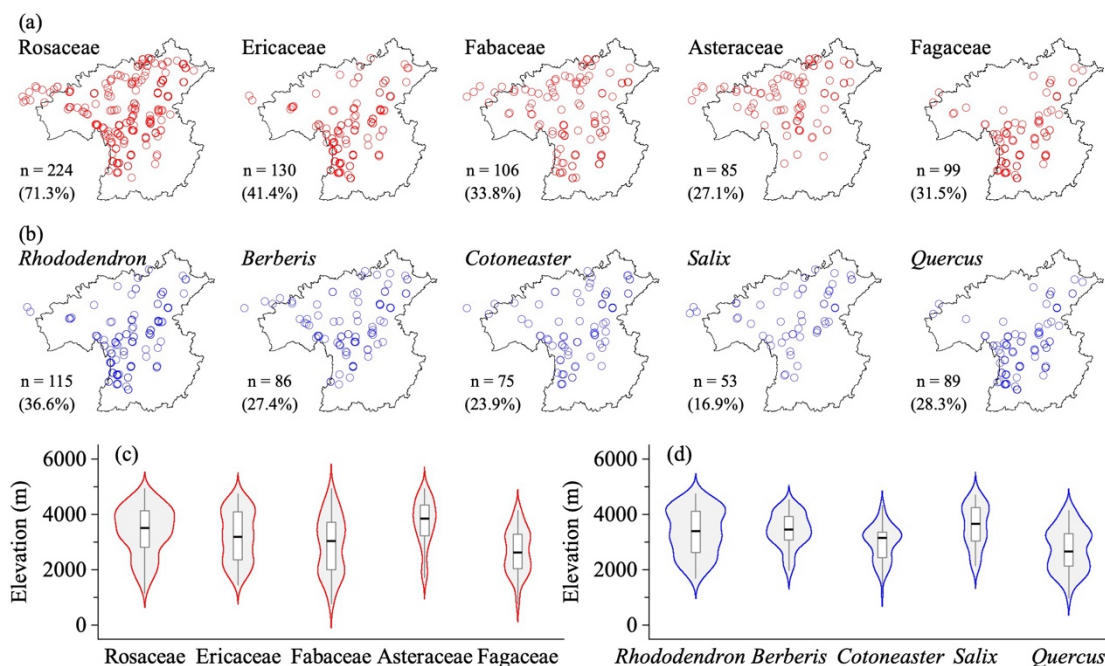
296 central parts, and are less frequent toward the northern sector. Asteraceae is more
 297 frequently recorded in the central and northern areas, but is sparse in the southernmost
 298 part (Fig. 3a). Along the elevational range surveyed, Rosaceae and Ericaceae show
 299 broad elevational distributions, with most records concentrated at middle to high
 300 elevations. Fabaceae spans the widest elevational ranges, extending from low valleys
 301 to alpine areas, but its distribution is mainly centered at low to middle elevations.
 302 Asteraceae is distinctly concentrated at high elevations, with a relatively high median
 303 elevation. In contrast, Fagaceae is mainly distributed at low to middle elevations and
 304 shows a lower elevational distribution center than the other dominant families (Fig. 3c).
 305 The five richest genera are *Rhododendron* (75 species), *Berberis* (34), *Cotoneaster* (30),
 306 *Salix* (24), and *Quercus* (22) (Table 2). *Rhododendron*, *Berberis*, and *Cotoneaster* are
 307 broadly distributed across the region, although their records are denser in the southern
 308 and central sectors. *Salix* is more frequent in the northern sector, whereas *Quercus* is
 309 mainly concentrated in the southern to central parts and becomes less frequent toward
 310 the north (Fig. 3b). *Rhododendron* and *Berberis* are mainly concentrated at middle to
 311 high elevations, *Cotoneaster* occupies a relatively broad middle-elevation range, *Salix*
 312 is centered at higher elevations, and *Quercus* shows the lowest elevational distribution
 313 center among the dominant genera, mainly occurring at low to middle elevations (Fig.
 314 3d).

315 **Table 2** Composition of dominant plant families and genera in the HDM-Plot dataset

	Dominant families	Dominant genera
All	Rosaceae (133, 11.8%)	<i>Rhododendron</i> (75, 6.7%)
	Ericaceae (93, 8.3%)	<i>Berberis</i> (34, 3.0%)
	Fabaceae (66, 5.9%)	<i>Cotoneaster</i> (30, 2.7%)
	Asteraceae (63, 5.6%)	<i>Salix</i> (24, 2.1%)
	Fagaceae (37, 3.3%)	<i>Quercus</i> (22, 2.0%)
Forest	Rosaceae (99, 13.4%)	<i>Rhododendron</i> (61, 8.3%)
	Ericaceae (78, 10.6%)	<i>Berberis</i> (30, 4.1%)
	Fabaceae & Fagaceae (34, 4.6%)	<i>Cotoneaster</i> (23, 3.1%)

	Berberidaceae (30, 4.1%)	<i>Quercus</i> (20, 2.7%)
	Pinaceae (28, 3.8%)	<i>Salix</i> (19, 2.6%)
Shrubland	Rosaceae (58, 18.1%)	<i>Rhododendron</i> (33, 10.3%)
	Ericaceae (38, 11.8%)	<i>Cotoneaster</i> (19, 5.9%)
	Fabaceae (25, 7.8%)	<i>Berberis</i> (16, 5.0%)
	Berberidaceae (17, 5.3%)	<i>Salix</i> (12, 3.7%)
	Lamiaceae (14, 4.4%)	<i>Lonicera</i> (11, 3.4%)
Grassland	Asteraceae (52, 19.5%)	<i>Gentiana</i> (18, 6.8%)
	Cyperaceae & Ranunculaceae (24, 9.0%)	<i>Kobresia</i> & <i>Saussurea</i> (12, 4.5%)
	Gentianaceae (19, 7.1%)	<i>Anaphalis</i> (10, 3.8%)
	Fabaceae & Rosaceae (18, 6.8%)	<i>Artemisia</i> (9, 3.4%)
	Poaceae (17, 6.4%)	<i>Anemone</i> & <i>Carex</i> (8, 3.0%)

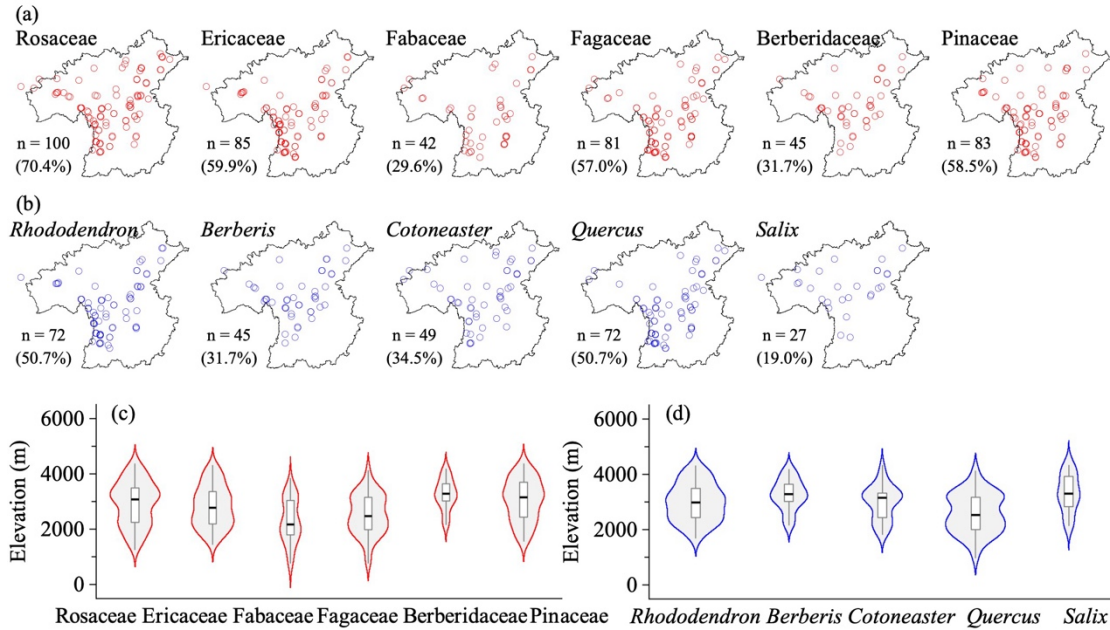
316 Dominant families and genera refer to the top five taxa ranked by number of species. An ampersand
 317 (&) connects families or genera with the same number of species. The values in parentheses indicate
 318 the number of species and its proportion of the total number of species in the corresponding category.



319
 320 **Figure 3.** Horizontal (a, b) and elevational (c, d) patterns of dominant plant families (a, c) and
 321 genera (b, d) in all vegetation plots in the HDM-Plot dataset. n denotes the number of plots in which
 322 each dominant family or genus was recorded, and values in parentheses indicate the proportion of
 323 the total survey plots.

324 Taxonomic composition differs among vegetation types (Table 2; Fig. 4–6). Forest

325 plots include 737 species, 238 genera, and 91 families (Table 1). The dominant families
326 are Rosaceae, Ericaceae, Fabaceae, Fagaceae, Berberidaceae, and Pinaceae (Table 2).
327 Rosaceae is mainly represented by shrub genera such as *Cotoneaster* (23.2%), *Rubus*
328 (13.1%), and *Rosa* (12.1%), as well as tree genera such as *Prunus* (14.1%). Ericaceae
329 is dominated by *Rhododendron* (78.2%), which is commonly shrubs and occasionally
330 small trees. Fabaceae contains a wide range of growth form, including shrub genera
331 (e.g., *Indigofera*, *Campylotropis*, and *Caragana*), climbers (mostly single-species
332 genera), and occasional tree taxa (e.g., *Dalbergia*). Fagaceae is composed of *Quercus*
333 (58.8%), *Lithocarpus* (20.6%), and *Castanopsis* (20.6%), and provides constructive
334 species in nearly one-third of forest plots. Berberidaceae only records one genus
335 *Berberis* and is a vital component of the shrub layer. Pinaceae offers the main needleleaf
336 constructive species in needleleaf forests and mixed forests, dominated by *Abies*
337 (35.7%), *Picea* (28.6%), *Larix* (10.7%), and *Pinus* (10.7%). Rosaceae, Ericaceae,
338 Fagaceae, Berberidaceae, and Pinaceae are widely recorded in forest plots, whereas
339 Fabaceae and Berberidaceae have lower plot frequencies and more restricted spatial
340 distributions (Fig. 4a). Rosaceae and Pinaceae occur across a broad part of the region,
341 while Ericaceae, Fabaceae, Fagaceae, and Berberidaceae are more concentrated in the
342 southern to central sectors. (Fig. 4a). Along the elevational gradient, Fabaceae and
343 Fagaceae are mainly distributed at low to middle elevations, although both extend
344 upward into middle-high elevational belts. Rosaceae and Ericaceae show broad middle-
345 elevation distributions. Berberidaceae and Pinaceae have higher elevational distribution
346 centers, with records mainly concentrated at middle to high elevations (Fig. 4c). The
347 top five genera are *Rhododendron*, *Berberis*, *Cotoneaster*, *Quercus*, and *Salix* (Table 2).
348 *Rhododendron*, *Berberis*, *Cotoneaster*, and *Quercus* are mainly recorded in the southern
349 to central parts of the study region, whereas *Salix* is more frequently recorded toward
350 the northern sector (Fig. 4b). *Quercus* has the lowest elevational distribution center and
351 is mainly concentrated at low to middle elevations, *Rhododendron* and *Cotoneaster*
352 occupy broad middle-elevation range. *Berberis* is more narrowly concentrated at
353 middle to high elevations, while *Salix* is centered at relatively high elevations among
354 the dominant forest genera (Fig. 4d).

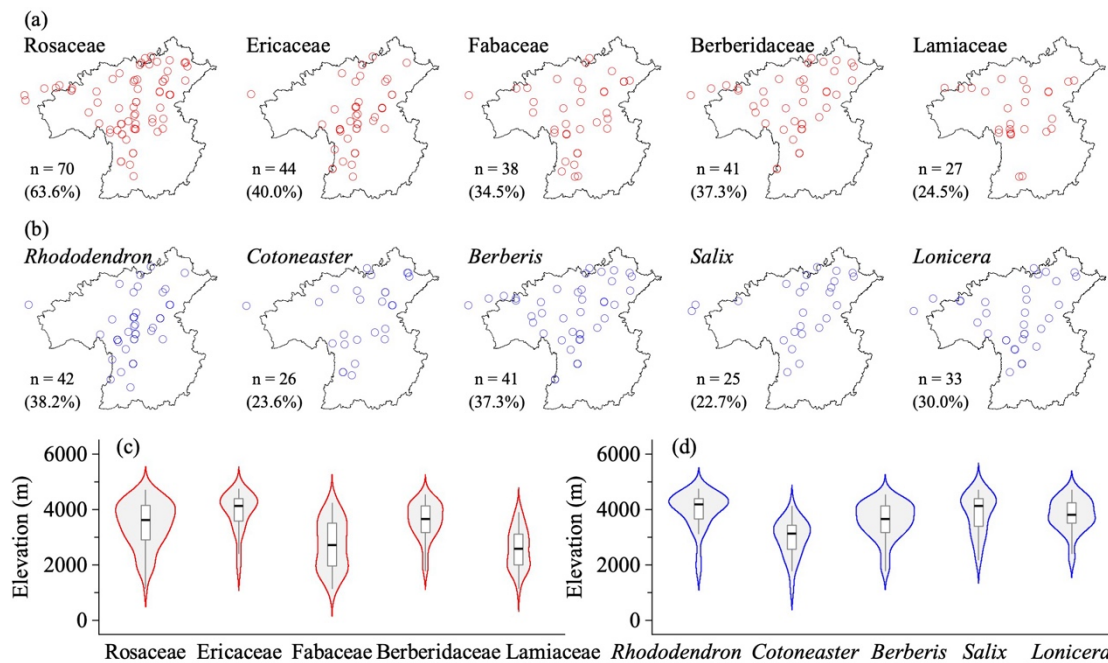


355

356 **Figure 4.** Horizontal (a, b) and elevational (c, d) patterns of dominant plant families (a, c) and
 357 genera (b, d) in forest vegetation plots in the HDM-Plot dataset. n denotes the number of plots in
 358 which each dominant family or genus was recorded, and the values in parentheses indicate the
 359 proportion of all forest plots.

360 110 shrubland plots survey a total of 321 species from 124 genera and 53 families
 361 (Table 1). Dominant families largely overlap with those of forests, with Lamiaceae as a
 362 new component. Rosaceae consists of *Cotoneaster* (32.8%), *Rosa* (15.5%), and *Spiraea*
 363 (13.8%) and forms the core of deciduous broadleaf shrublands. Ericaceae is strongly
 364 dominated by *Rhododendron* (86.8%) and typically acts as the constructive species in
 365 evergreen broadleaf shrublands. Fabaceae includes *Caragana* (20.0%), *Campylotropis*
 366 (16.0%), and *Indigofera* (16.0%), commonly recorded in the dry-hot valley shrublands.
 367 Berberidaceae is almost represented by *Berberis* (94.1%), with *Mahonia* recorded but
 368 not in forest plots. Lamiaceae is characterized by typical dry-hot valley genera such as
 369 *Caryopteris* (28.6%), *Isodon* (21.4%), and *Elsholtzia* (21.4%). Rosaceae is the most
 370 widely distributed shrubland family across the study region, whereas Fabaceae and
 371 Berberidaceae are also broadly recorded. Ericaceae is more concentrated in the southern
 372 to northwestern sectors, and Lamiaceae are mainly distributed in the north (Fig. 5a).
 373 Ericaceae has the highest elevational distribution center and is mainly concentrated in
 374 high elevations, and Berberidaceae is also mainly distributed at middle to high
 375 elevations. Rosaceae spans a broad elevational range but is denser at middle to high

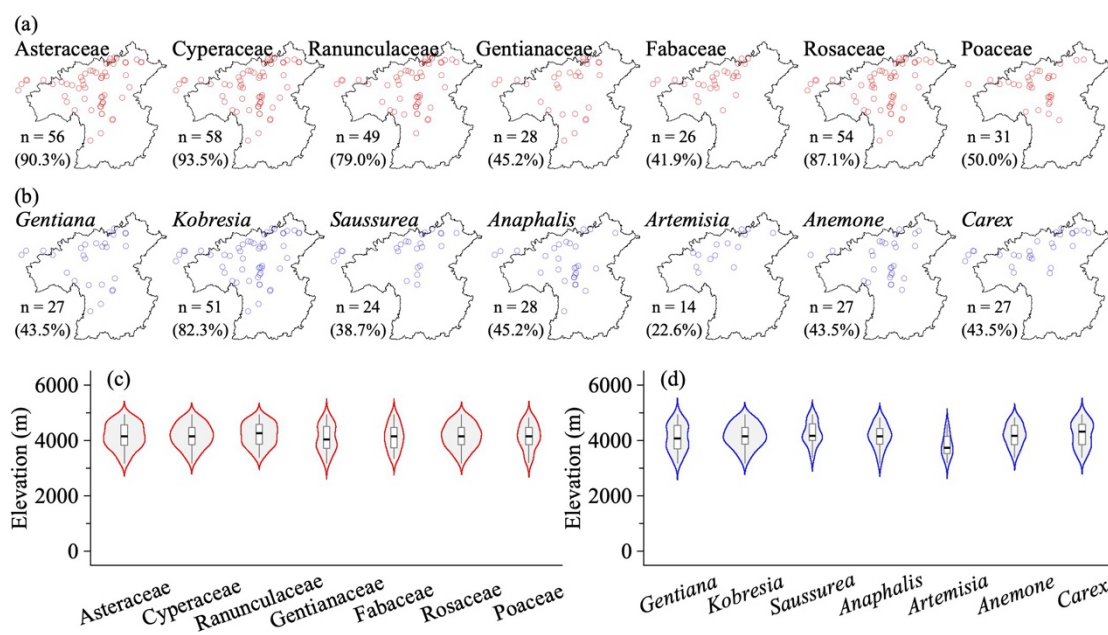
376 elevations, while Fabaceae and Lamiaceae have lower elevational distribution centers
 377 and are mainly concentrated at low to middle elevations (Fig. 5c). The top genera are
 378 *Rhododendron*, *Cotoneaster*, *Berberis*, *Salix*, and *Lonicera* (Table 2). *Berberis* and
 379 *Lonicera* are widely distributed across the region, whereas *Rhododendron*, *Cotoneaster*,
 380 and *Salix* are primarily aligned along a southwest–northeast direction (Fig. 5b). Their
 381 elevational distributions are also distinct. *Rhododendron* and *Salix* are concentrated at
 382 high elevations, with higher median elevations and relatively narrow central
 383 distributions. *Berberis* and *Lonicera* are mainly distributed at middle to high elevations.
 384 *Cotoneaster* has a lower elevational distribution center, and is mainly concentrated at
 385 middle elevations (Fig. 5d).



386
 387 **Figure 5.** Horizontal (a, b) and elevational (c, d) patterns of dominant plant families (a, c) and
 388 genera (b, d) in shrubland vegetation plots in the HDM-Plot dataset. n denotes the number of plots
 389 in which each dominant family or genus was recorded, and the values in parentheses indicate the
 390 proportion of all shrubland plots.

391 62 grassland plots investigate a total of 266 species belonging to 38 families and
 392 113 genera (Table 1). The most species-rich families are Asteraceae, Cyperaceae,
 393 Ranunculaceae, Gentianaceae, Fabaceae, Rosaceae, and Poaceae (Table 2). Asteraceae
 394 is largely represented by *Saussurea* (23.1%), *Anaphalis* (19.2%), *Artemisia* (17.3%),
 395 and *Taraxacum* (13.5%), consisting of perennial forbs and semi-shrubs that contribute
 396 to forb grasslands. Cyperaceae is dominated by tussock *Kobresia* and rhizome *Carex*

397 and provide the main constructive species in grassland vegetation (42 plots), especially
 398 the zonal species *K. pygmaea*. Ranunculaceae is represented by *Anemone* (33.3%) and
 399 *Ranunculus* (20.8%), Gentianaceae is strongly dominated by *Gentiana* (94.7%), and
 400 Fabaceae is composed of *Astragalus* (33.3%) and *Oxytropis* (27.8%). Rosaceae consists
 401 of perennial herbs such as *Argentina* (33.3%) and *Potentilla* (22.2%) and dwarf shrub
 402 *Dasiphora* (11.1%). Poaceae is dominated by tussock grasses, including *Poa* (17.6%),
 403 *Aristida* (17.6%), *Stipa* (11.8%), and *Festuca* (11.8%). The dominant grassland families
 404 are mainly distributed in the central and northern parts of the HDM-Plot study region
 405 (Fig. 6a). Asteraceae, Cyperaceae, Ranunculaceae, Rosaceae, and Poaceae are broadly
 406 recorded across grassland plots, whereas Gentianaceae and Fabaceae have relatively
 407 lower plot frequencies (Fig. 6a). Their elevational distributions are concentrated in
 408 high-elevation belts, but with slight differences in distribution centers and ranges (Fig.
 409 6c). The dominant genera include *Gentiana*, *Kobresia*, *Saussurea*, *Anaphalis*, *Artemisia*,
 410 *Anemone*, and *Carex* (Table 2). *Kobresia* is the most broadly distributed dominant
 411 grassland genus across both horizontal space and the elevational gradient, consistent
 412 with its role as a major alpine meadow constructive genus (Fig. 6b, d). *Gentiana*,
 413 *Saussurea*, *Anaphalis*, *Anemone*, and *Carex* are also mainly concentrated in high-
 414 elevation grasslands, whereas *Artemisia* shows a relatively narrower and slightly lower
 415 elevational distribution compared with the other dominant genera (Fig. 6d).

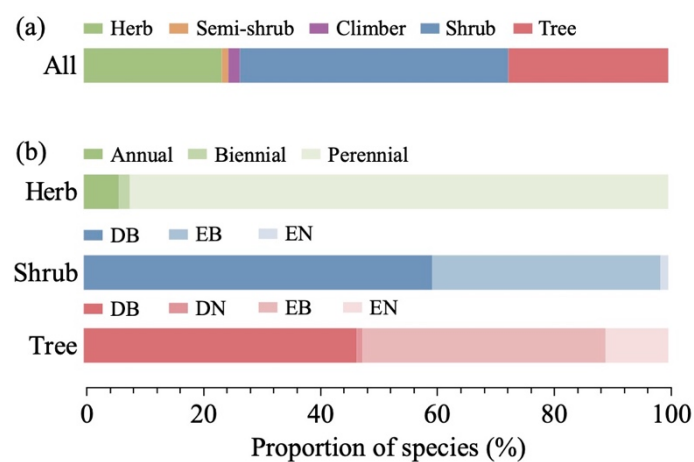


416

417 **Figure 6.** Horizontal (a, b) and elevational (c, d) patterns of dominant plant families (a, c) and
 418 genera (b, d) in grassland vegetation plots in the HDM-Plot dataset. n denotes the number of plots
 419 in which each dominant family or genus was recorded, and the values in parentheses indicate the
 420 proportion of all grassland plots.

421 4.2 Growth forms and life forms

422 The 1,127 species in the HDM-Plot dataset can be categorized into five growth forms
 423 (Fig. 7a). Shrubs comprise the largest proportion of recorded species (46.0%), followed
 424 by trees (27.3%) and herbs (23.6%), while climbers (2.0%) and semi-shrubs (1.2%)
 425 contribute a small number of species (Fig. 7a). Among herbs, perennials dominate
 426 (92.1%), while annuals (6.0%) and biennials (1.9%) are comparatively rare (Fig. 7b).
 427 Woody species show clear contrasts in leaf type and phenology (Fig. 7b). Shrubs are
 428 almost composed of broadleaf (98.7%), with deciduous shrubs (59.7%) more frequent
 429 than evergreen shrubs (40.4%), whereas trees exhibit a higher proportion of needleleaf
 430 species (11.7%) and a near balance between evergreen (52.3%) and deciduous (47.8%)
 431 species (Fig. 7b).

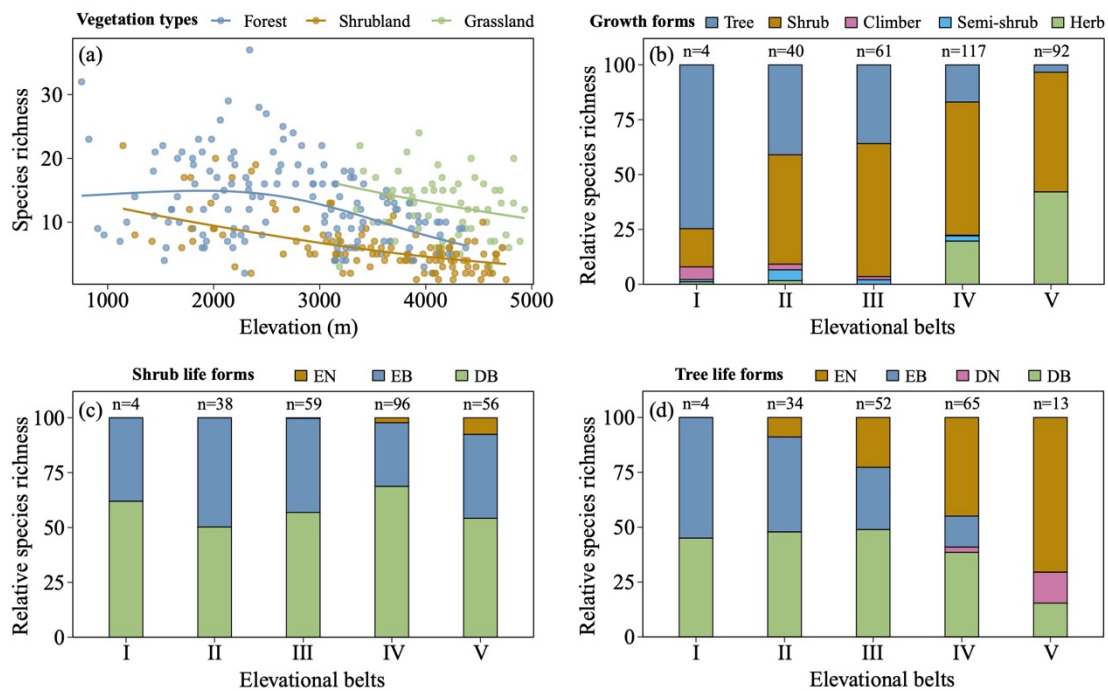


432 **Figure 7.** Growth-form composition of all species (a) and life-form composition within herbaceous,
 433 shrub, and tree species (b) surveyed in the HDM-Plot dataset. Bars show the proportion of species
 434 in each category. DB, deciduous broadleaf; DN, deciduous needleleaf; EB, evergreen broadleaf; and
 435 EN, evergreen needleleaf.
 436

437 In the HDM-Plot study region, plot-level species richness shows distinct
 438 elevational trends among vegetation types after accounting for plot area (Fig. 8a). Forest
 439 plots maintain relatively high species richness from low to middle elevations, followed
 440 by a decline toward higher elevations. Shrubland plots show a decreasing trend along
 441 the elevational gradient. Grassland plots are restricted to middle- and high-elevation

442 belts, with relatively high richness at the lower part of their observed elevational range
 443 and a gradual decline toward higher elevations.

444 Growth-form composition varies clearly across elevational belts in surveyed plots
 445 (Fig. 8b). Trees dominate the lowest elevational belt and decline with increasing
 446 elevation. Shrubs remain the major component from low-middle to high elevations and
 447 are especially prominent in the middle-elevation belts. Herbs increase strongly toward
 448 the highest elevational belt. Woody life-form composition also shifts with elevation (Fig.
 449 8c, d). For shrubs, deciduous broadleaf shrubs dominate most elevational belts, whereas
 450 evergreen broadleaf shrubs contribute substantially across the elevational gradient,
 451 particularly from low to middle elevations. Evergreen needleleaf shrubs are absent or
 452 rare at lower elevations and occur mainly in the upper elevational belts (Fig. 8c). Tree
 453 life forms show stronger elevational turnover (Fig. 8d). Evergreen broadleaf trees are
 454 more common at low elevations and decrease sharply toward higher elevations.
 455 Deciduous broadleaf trees contribute substantially from low to middle-high elevations
 456 but decline in the highest belt. Evergreen needleleaf trees increase with elevation and
 457 become dominant in the upper belts. Deciduous needleleaf trees are largely restricted
 458 to high-elevation belts (Fig. 8d).



459
 460 **Figure 8.** Elevational patterns of plot-level species richness (a), growth forms (b), and woody life
 461 forms (c, d) in the HDM-Plot dataset. In panel (a), points represent observed species richness in

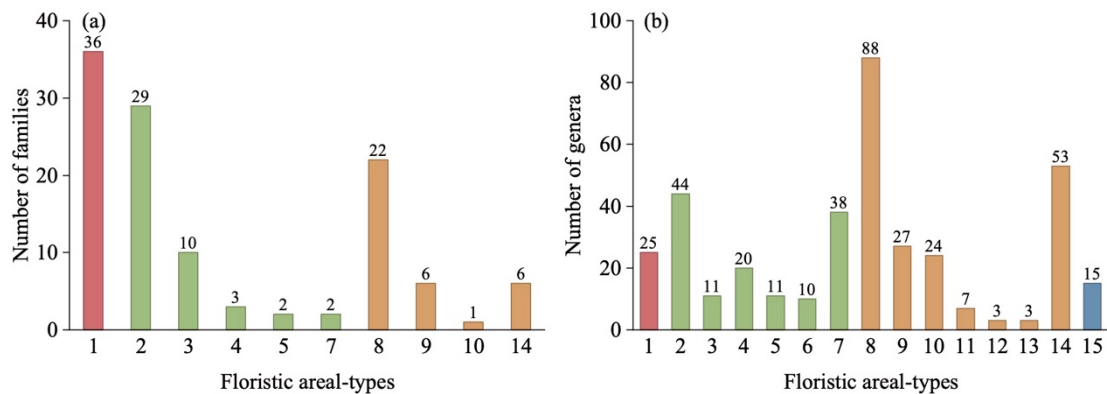
462 individual plots, and fitted lines show elevational trends estimated using generalized additive
463 models with plot area included as a covariate. Predictions were standardized to representative plot
464 areas of 100 m² for forests, 25 m² for shrublands, and 1 m² for grasslands. Panels (b–d) show mean
465 plot-level proportions within each elevational belt. Elevational belts are defined as I, 0–1000 m; II,
466 1000–2000 m; III, 2000–3000 m; IV, 3000–4000 m; and V, 4000–5000 m. n denotes the number of
467 plots included in each elevational belt. DB, deciduous broadleaf; DN, deciduous needleleaf; EB,
468 evergreen broadleaf; and EN, evergreen needleleaf.

469 **4.3 Floristic characteristics**

470 At the family level, 117 families can be assigned to 10 areal-type categories (Fig.
471 9a). Cosmopolitan families account for 30.8% of the total, tropical families for 39.3%,
472 and temperate families for 29.9%. Pantropic families comprise the largest share within
473 tropical families (63.0%), with species-rich families including Lauraceae, Sapindaceae,
474 Celastraceae, Euphorbiaceae, and Anacardiaceae. North temperate families account for
475 62.9% of the temperate component, represented by Ericaceae, Fagaceae, Berberidaceae,
476 Salicaceae, and Pinaceae. These patterns reflect that the floristic composition of the
477 HDM-Plot study region retains a tropical–subtropical elements and also incorporating
478 temperate–alpine attributes.

479 At the genus level, 379 genera can be assigned into 15 areal-type categories (Fig.
480 9b). Temperate genera dominate (54.1%), followed by tropical genera (35.4%), whereas
481 cosmopolitan (6.6%) and Chinese endemic genera (4.0%) are less frequent. Temperate
482 genera are mainly north temperate (42.9%), represented by *Rhododendron*, *Berberis*,
483 *Cotoneaster*, *Salix*, and *Quercus*. For tropical genera, pantropical (32.8%) and tropical
484 Asian (28.4%) areal-types are most common, with *Ilex* and *Indigofera* as pantropical
485 representatives and *Fargesia*, *Leptodermis*, *Caryopteris*, and *Corylopsis* as East Asian
486 representatives. Compared with the family level, the genus level composition shows a
487 clear shift toward temperate elements. However, when the number of species contained
488 in each areal-type group is considered, temperate genera account for 66.7% of the
489 recorded species, whereas tropical genera account for 23.3% (Table S2). A plot–genus
490 occurrence analysis further shows that temperate genera dominate plot-level occurrence
491 records and are mainly associated with high elevations, whereas tropical genera are
492 more closely associated with low elevations (Fig. S2). Both temperate and tropical

493 genera are spatially widespread within the study region, but the number of plot-level
 494 occurrence records of temperate genera is nearly four times that of tropical genera (Fig.
 495 S2). Therefore, the dataset records transitional floristic features across the Hengduan
 496 Mountains and adjacent regions, while temperate elements remain dominant when
 497 species representation and plot-level occurrence are considered.



498

499 **Figure 9.** Floristic areal-types of plant families **(a)** and genera **(b)** surveyed in the HDM-Plot dataset.
 500 1, Cosmopolitan; 2, Pantropic; 3, Tropical Asia & Tropical America disjuncted; 4, Old World
 501 Tropics; 5, Tropical Asia & Tropical Australasia; 6, Tropical Asia to Tropical Africa; 7, Tropical
 502 Asia (Indo–Malaysia); 8, North Temperate; 9, East Asia & North America disjuncted; 10, Old World
 503 Temperate; 11, Temperate Asia; 12, Mediterranean, West Asia to Central Asia; 13, Central Asia; 14,
 504 East Asia; and 15, Endemic to China (Wu, 1991, 2003). Bar colors indicate four floristic areal-type
 505 groups: cosmopolitan (red), tropical (green), temperate (orange), and endemic to China (blue).

506 4.4 Vegetation classification

507 Based on field surveys and the *revised vegetation classification system of China*
 508 (Guo et al., 2020), 314 plots can be classified into three vegetation formation groups,
 509 namely forest, shrubland, and grassland (Fig. 10; Table S4). These plots can be further
 510 classified into 18 vegetation formations, 142 alliance groups, 209 alliances, 238
 511 association groups, and 299 associations (Table S4). Because these lower-level units
 512 are highly detailed and many are represented by only one plot, the full hierarchical
 513 classification is provided in Table S4 and in the published dataset, whereas the main
 514 text focuses on vegetation formation groups and vegetation formations (Fig. 10; Table
 515 3).

516 Forest vegetation formation group includes eight vegetation formations: deciduous

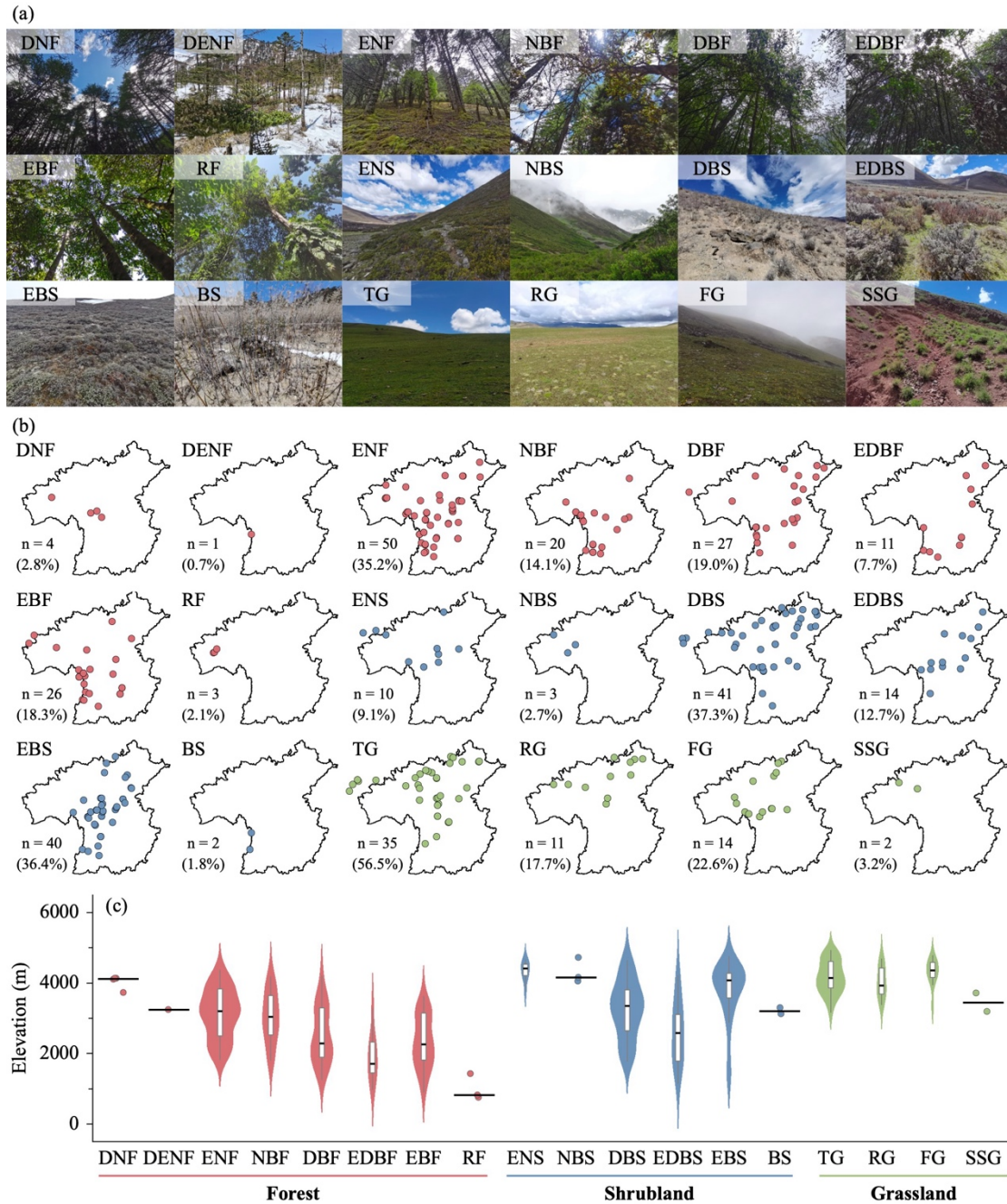
517 needleleaf forest (DNF), mixed deciduous and evergreen needleleaf forest (DENF),
518 evergreen needleleaf forest (ENF), mixed needleleaf and broadleaf forest (NBF),
519 deciduous broadleaf forest (DBF), mixed evergreen and deciduous broadleaf forest
520 (EDBF), evergreen broadleaf forest (EBF), and rainforest (RF) (Table S4). DNF
521 includes only one alliance (*Larix potaninii* var. *macrocarpa*) and appears at 3,732–
522 4,136 m in the central and northwestern study region. It has 10 ± 2 species per plot,
523 community height of 10.5 ± 3.9 m, coverage of $71 \pm 13\%$, and mean DBH of 11.9 ± 5.1
524 cm. DENF is also rare and was recorded from a single plot in Fugong (western border
525 between China and Myanmar) at 3,247 m. This plot contains 4 species, community
526 height of 15.6 m, coverage of 35%, and mean DBH of 10.1 cm. ENF is widespread
527 throughout the study region at 1,809–4,377 m and is constructed by *Pinus*, *Abies*, *Picea*,
528 *Juniperus*, and *Tsuga*. It includes 12 ± 6 species per plot, community height of $16.7 \pm$
529 7.4 m, coverage of $66 \pm 14\%$, and mean DBH of 17.1 ± 11.6 cm. NBF is concentrated
530 in the southern study region at 1,801–4,189 m and typically combines *Pinus*, *Abies* and
531 *Picea* with broadleaf trees such as *Quercus*, *Alnus*, and *Lithocarpus*. This formation
532 records 14 ± 7 species per plot, community height of 18.9 ± 6.4 m, coverage of $68 \pm$
533 17% , and mean DBH of 16.1 ± 7.9 cm. DBF is widely distributed at 1,256–4,217 m,
534 excluding the northwestern study region, and is commonly constructed by *Alnus*, *Betula*,
535 *Quercus*, and *Populus*. The corresponding plot-level values are 14 ± 7 species per plot,
536 13.1 ± 5.5 m in community height, $76 \pm 13\%$ in coverage, and 10.2 ± 5.8 cm in mean
537 DBH. EDBF occurs patchily from the southwestern to northeastern study region at 966–
538 3,298 m, where evergreen components mainly *Quercus* and *Castanopsis* co-occur with
539 deciduous broadleaf taxa such as *Alnus*. It has 15 ± 6 species per plot, community height
540 of 14.8 ± 6.4 m, coverage of $73 \pm 10\%$, and mean DBH of 10.7 ± 5.5 cm. EBF is
541 widespread at low to middle elevations (906–3,636 m) in the study region and is most
542 frequently constructed by *Quercus*. This formation surveys 12 ± 5 species per plot, 14.7
543 ± 8.8 m in community height, $74 \pm 16\%$ in coverage, and 15.4 ± 8.8 cm in mean DBH.
544 RF is restricted to the lowest elevations in Medog, northwestern part of the study region
545 (754–1,431m) and is characterized by tropical and subtropical trees. RF plots contain
546 24 ± 7 species per plot, community height of 35.3 ± 11.9 m, coverage of $80 \pm 10\%$, and

547 mean DBH of 23.3 ± 10.9 cm (Fig. 10; Table 3).

548 Shrubland vegetation formation group can be further divided into six vegetation
549 formations: evergreen needleleaf shrubland (ENS), needleleaf and broadleaf shrubland
550 (NBS), deciduous broadleaf shrubland (DBS), evergreen and deciduous broadleaf
551 shrubland (EDBS), evergreen broadleaf shrubland (EBS), and bamboo shrubland (BS)
552 (Table S4). ENS consists of two alliances (*Juniperus squamata* and *J. convallium*) and
553 occurs mainly along the central and northwestern margin of the study region at 3,757–
554 4,668 m. ENS plots have 5 ± 2 species per plot, community height of 2.5 ± 2.3 m,
555 coverage of $78 \pm 18\%$, and mean BD of 3.4 ± 1.8 cm. NBS is rare and was surveyed
556 from high-elevational area (4,044–4,720 m) in Chamdo, northwestern part of the study
557 region, where *Juniperus* co-occurs with broadleaf shrubs including *Ribes*, *Salix*, and
558 *Spiraea*. Its plot-level values are 6 ± 1 species per plot, 2.4 ± 1.0 m in community height,
559 $60 \pm 33\%$ in coverage, and 2.6 ± 1.6 cm in mean BD. DBS is widespread across the
560 study region at 1,772–4,662 m and is most frequently dominated by *Berberis*, *Salix*,
561 *Rosa*, *Cotoneaster*, and *Sibiraea*. This formation includes 7 ± 4 species per plot,
562 community height of 2.7 ± 1.7 m, coverage of $61 \pm 21\%$, and mean BD of 1.6 ± 0.6 cm.
563 EDBS spans a broad elevational gradient (1,144–4,226 m) from the central to
564 northeastern study region and features mixtures of evergreen (e.g., *Rhododendron* and
565 *Daphne*) with deciduous components (e.g., *Rosa* and *Zanthoxylum*). EDBS plots
566 contain 10 ± 6 species per plot, community height of 3.6 ± 3.1 m, coverage of $62 \pm 22\%$,
567 and mean BD of 1.9 ± 1.2 cm. EBS is widely distributed from the southwestern to
568 northeastern study region at 1,257–4,758 m and is commonly dominated by
569 *Rhododendron* and *Quercus*. It has 5 ± 4 species per plot, community height of $2.5 \pm$
570 2.3 m, coverage of $69 \pm 17\%$, and mean BD of 1.6 ± 1.1 cm. BS is uncommon in the
571 dataset and was found in Yunnan Province at 3,120–3,290 m and includes two alliances
572 (*Fargesia gongshanensis* and *F. melanostachys*). BS plots record 5 ± 4 species per plot,
573 community height of 5.4 ± 2.9 m, coverage of $68 \pm 11\%$, and mean BD of 2.7 ± 1.1 cm
574 (Fig. 10; Table 3).

575 Grassland vegetation formation group comprises four vegetation formations:
576 tussock grassland (TG), rhizome grassland (RG), forb grassland (FG), and semi-shrub

577 grassland (SSG) (Table S4). TG is widespread across the study region at 3,168–4,932
578 m and is strongly dominated by *Kobresia*, especially the widespread alpine meadow
579 species *K. pygmaea* (24 plots). This formation has 12 ± 4 species per plot, community
580 height of 0.061 ± 0.033 m, and coverage of $81 \pm 15\%$. RG occurs mainly in the northern
581 study region at 3,379–4,701 m and is represented by *Carex*, with *C. enervis* frequently
582 recorded. It contains 14 ± 5 species per plot, community height of 0.108 ± 0.102 m, and
583 coverage of $79 \pm 25\%$. FG is concentrated from the central to northern study region at
584 3,345–4,784 m and is characterized by forb constructed communities, with *Argentina*
585 as a common genus. Its plot-level values are 11 ± 6 species per plot, 0.079 ± 0.055 m
586 in community height, and $77 \pm 16\%$ in coverage. SSG is rare and has a single alliance
587 (*Artemisia vestita*), observed in dry-hot valleys in the northwestern study region at
588 3,186–3,710 m. The alliance has 5 ± 3 species per plot, community height of $0.300 \pm$
589 0.283 m, and coverage of $50 \pm 28\%$ (Fig. 10; Table 3).



590

591 **Figure 10.** Representative photographs (a), horizontal distribution (b), and elevational distribution
 592 (c) of vegetation formations in the HDM-Plot dataset. Red, blue, and green points represent forest,
 593 shrubland, and grassland formations, respectively. n denotes the number of plots for each vegetation
 594 formation, and values in parentheses indicate the proportion of the corresponding formation group.
 595 Violin plots with embedded boxplots are shown for vegetation formations represented by at least
 596 five plots, whereas formations with fewer than five plots are displayed as individual points only.
 597 Black horizontal lines reflect median elevation. DNF, deciduous needleleaf forest; DENF, mixed
 598 deciduous and evergreen needleleaf forest; ENF, evergreen needleleaf forest; NBF, mixed needleleaf
 599 and broadleaf forest; DBF, deciduous broadleaf forest; EDBF, mixed evergreen and deciduous
 600 broadleaf forest; EBF, evergreen broadleaf forest; RF, rainforest; ENS, evergreen needleleaf
 601 shrubland; NBS, needleleaf and broadleaf shrubland; DBS, deciduous broadleaf shrubland; EDBS,
 602 evergreen and deciduous broadleaf shrubland; EBS, evergreen broadleaf shrubland; BS, bamboo

603 shrubland; TG, tussock grassland; RG, rhizome grassland; FG, forb grassland; and SSG, semi-
 604 shrubby grassland.

605 **Table 3** Summary of community characteristics and structure in the HDM-Plot dataset

Formations	SR	Community height (m)	Community Coverage (%)	DBH or BD (cm)
DNF	10 ± 2	10.5 ± 3.9	71 ± 13	11.9 ± 5.1
DENF	4	15.6	35	10.1
ENF	12 ± 6	16.7 ± 7.4	66 ± 14	17.1 ± 11.6
NBF	14 ± 7	18.9 ± 6.4	68 ± 17	16.1 ± 7.9
DBF	14 ± 7	13.1 ± 5.5	76 ± 13	10.2 ± 5.8
EDBF	15 ± 6	14.8 ± 6.4	73 ± 10	10.7 ± 5.5
EBF	12 ± 5	14.7 ± 8.8	74 ± 16	15.4 ± 8.8
RF	24 ± 7	35.3 ± 11.9	80 ± 10	23.3 ± 10.9
ENS	5 ± 2	2.5 ± 2.3	78 ± 18	3.4 ± 1.8
NBS	6 ± 1	2.4 ± 1.0	60 ± 33	2.6 ± 1.6
DBS	7 ± 4	2.7 ± 1.7	61 ± 21	1.6 ± 0.6
EDBS	10 ± 6	3.6 ± 3.1	62 ± 22	1.9 ± 1.2
EBS	5 ± 4	2.5 ± 2.3	69 ± 17	1.6 ± 1.1
BS	5 ± 4	5.4 ± 2.9	68 ± 11	2.7 ± 1.1
TG	12 ± 4	0.061 ± 0.033	81 ± 15	/
RG	14 ± 5	0.108 ± 0.102	79 ± 25	/
FG	11 ± 6	0.079 ± 0.055	77 ± 16	/
SSG	5 ± 3	0.300 ± 0.283	50 ± 28	/

606 Values are summarized at the plot level within each vegetation formation and are shown as mean ±
 607 SD. SR denotes species richness per plot. DBH or BD represents the mean diameter at breast height
 608 or basal diameter of woody species within each plot.

609 **5 Data availability**

610 The HDM-Plot dataset includes two components: a plot dataset and a habitat photo
 611 dataset. The plot dataset is provided as a Microsoft Excel format containing six sheets:
 612 1) summary (Table 4); 2) basic plot information; 3) raw plot survey data; 4) species list;

613 5) species important values; and 6) vegetation classification. The habitat photo dataset
614 is organized by survey period (i.e., 202203, 202205, 2023, and 2024). Photo files are
615 provided in JPG format, named by plot ID, and correspond to the plots in the dataset.
616 The dataset is publicly available from Figshare (Jin et al., 2026a;
617 <https://doi.org/10.6084/m9.figshare.32706207>) and through the National Tibetan
618 Plateau / Third Pole Environment Data Center (Jin et al., 2026b;
619 <https://doi.org/10.11888/Terre.tpd.c.303394>).

620 **Table 4** Summary information of the HDM-Plot dataset.

Heading	Description	Type
Plot No	Plot number based on survey time	Code
Province	Administrative province of the plot location	Character
Longitude (°E)	Longitude in decimal degrees by GPS	Numeric
Latitude (°N)	Latitude in decimal degrees by GPS	Numeric
Elevation (m)	Elevation in decimal degrees by GPS	Integer
Disturbance intensity	Degree of disturbance recorded in the survey	Character
Plot size (m × m)	Plot size = plot length × plot width	Character
Community height (m)	Maximum height of the dominant vegetation layer within a plot	Numeric
Community coverage (%)	Total vegetation coverage of the plot	Integer
Species richness	Number of species recorded in the plot	Integer
Latin name	Scientific name of the species (Flora of China, FOC)	Character
Growth form	Tree, shrub, climber, semi-shrub, and herb	Character
Phenological period	Phenological stage during survey (e.g., leaf period)	Character
Number of plants (clusters)	Number of individuals or clumps recorded	Integer
Height (m)	Leaf-layer height (herb) / canopy height (woody)	Numeric
FBH (cm)	Reproductive branch height (herb)	Numeric
BD (cm)	Base diameter	Numeric
DBH (cm)	Diameter at breast height	Numeric
Crown a (m)	Maximum crown width (woody)	Numeric

Crown b (m)	Crown width perpendicular to maximum axis (woody)	Numeric
Coverage (%)	Specific species coverage (herb)	Numeric
Plant status	Vitality status of the individual (e.g., dead wood)	Character
Chinese name	Chinese name of the species (FOC)	Character
Genus	Genus of the species (FOC)	Character
Family	Family of the species (FOC)	Character
Leaf phenology	Deciduous vs. Evergreen	Character
Leaf type	Broadleaf vs. needleleaf	Character
Life span	Annual, biennial, and perennial	Character
No. of plots observed	Number of plots in which the species was recorded	Integer
Layer	Vegetation layer (e.g., tree layer)	Character
IV (%)	Importance value of the species within the plot	Numeric
Vegetation formation group	Supplementary upper-level unit (e.g., forest)	Character
Vegetation formation	Upper-level unit (e.g., evergreen needleleaf forest)	Character
Alliance group	Supplementary middle-level unit (e.g., <i>Abie</i> forest)	Character
Alliance	Middle-level unit (e.g., <i>A. georgei</i> forest)	Character
Association group	Supplementary lower-level unit (e.g., <i>A. georgei</i> - shrub forest)	Character
Association	Lower-level unit (<i>A. georgei</i> - <i>Rubus amabilis</i> forest)	Character

621 **6 Summary**

622 The HDM-Plot dataset was compiled from four extensive fieldworks conducted
623 by our research group between 2022 and 2024. It provides detailed raw records from
624 314 vegetation plots spanning major vegetation types in the HDM and adjacent regions,
625 from low-elevational dry-hot valleys to subalpine and alpine areas. The dataset offers a
626 robust, standardized data for studies of vegetation ecology, conservation planning, and
627 ecological restoration in this biodiversity hotspot, and provides an important regional
628 complement to global vegetation plot compilations such as the sPlot (Sabatini et al.,
629 2021), which rarely include the vegetation plots from southwestern China and the

630 Tibetan Plateau. The localized vegetation plot dataset can be integrated into existing
631 global plot database of sPlot, and further contributes to large-scale synthesis.

632 Several limitations remain due to the challenging field conditions and constraints
633 in manpower and resources. First, although the surveyed plots cover broad vegetation
634 types, climatic space, and elevational gradients (Fig. 2), the study region, especially the
635 HDM has extremely complex topography and highly heterogeneous vegetation, and
636 steep terrain often prevented the establishment of fully standardized plots. As a result,
637 plot size could not always be kept uniform, and plot distribution may be uneven in some
638 areas, which can affect representativeness and comparability. Second, given the high
639 diversity and strong spatial turnover of species composition, individual plots may not
640 fully capture the regional variability, potentially producing sampling bias. Third, some
641 plot attributes, such as plant height, crown width, and coverage, were visually estimated
642 in the field and may therefore be subject to observer uncertainty. Nevertheless, these
643 limitations should be viewed in the context of field-based vegetation surveys in a
644 topographically complex and highly heterogeneous mountain region. Assembling a
645 large, structurally detailed plot dataset under harsh field conditions represents a vital
646 contribution. More importantly, we believe that the dataset remains a valuable
647 community resource for large-scale mountain vegetation studies, as it provides
648 standardized and openly accessible plot-level records from highly heterogeneous and
649 relatively underrepresented mountain region. We expect the HDM-Plot dataset to
650 provide a valuable reference for ongoing and future efforts of vegetation reassessment
651 and ecological research across the region.

652 Compared with our previously published dataset on the Tibetan Plateau (Jin et al.,
653 2022), the HDM-Plot dataset fills a key geographic gap on the southeastern Plateau and
654 demonstrates enhanced representativeness about plot distribution, species richness, and
655 vegetation types. Plots are not restricted to areas along major roads, but also extend into
656 accessible valleys and pathways. This is the first comprehensive vegetation plot dataset
657 for the HDM and adjacent regions to our knowledge with broad spatial coverage and
658 representation of diverse vegetation types. In addition to raw species composition
659 records, the dataset provides standardized geographic coordinates, species list, and

660 hierarchical vegetation classifications.

661 The vegetation classification in the HDM-Plot dataset follows the revised
662 vegetation classification system of China (Guo et al., 2020), emphasizing field-based
663 community physiognomy, vertical structure, constructive species, and species
664 importance values. This approach provides a field-based and nationally consistent
665 framework for vegetation classification and future comparison with the *Vegegraphy of*
666 *China*. During vegetation classification, we observed shrubland communities in which
667 co-constructive species differ in leaf type and phenology, analogous to mixed forests.
668 For example, shrublands jointly dominated by *Juniperus* and *Rhododendron* combine
669 needleleaf and broadleaf components and may include evergreen and deciduous
670 elements. Accordingly, we introduced two shrubland vegetation formations within the
671 Guo et al. (2020) scheme: (a) needleleaf and broadleaf shrubland, and (b) evergreen and
672 deciduous broadleaf shrubland. Similarly, in grasslands, co-constructive species often
673 belong to different functional groups (e.g., tussock, rhizome, and forb), which are not
674 always clearly separated in the current classification framework. We therefore retained
675 multiple co-constructive species in alliance naming, while identifying the vegetation
676 formation according to the life form of the species with the highest IV. For example,
677 *Kobresia pygmaea* + *Potentilla saundersiana* grassland alliance was classified as a
678 tussock grassland vegetation formation.

679 As a complementary assessment, we further numerically classified vegetation
680 from the HDM-Plot dataset based on species composition using TWINSpan (Fig. S3).
681 The first division broadly separated alpine grassland plots from non-alpine grassland
682 plots, consistent with the major physiognomic contrast in the dataset. However, finer
683 divisions did not always correspond to the field-based vegetation formations, probably
684 reflecting local species turnover, rare taxa, and uneven sampling among vegetation
685 types. Therefore, quantitative classification provides a useful complementary
686 perspective, but the field-based classification following Guo et al. (2020) remains the
687 primary framework for this data paper. These plot-based findings and standardized data
688 provide support for the ongoing revision of China's vegetation classification system
689 (Guo et al., 2020) and for the update of *Vegegraphy of China* (Fang et al., 2020). The

690 ecological environment of southwestern China is highly fragile and increasingly
691 exposed to human pressures, with limited capacity for natural recovery. Updated and
692 standardized baseline data is therefore essential for guiding conservation, ecological
693 planning, and restoration strategies, and for supporting biodiversity assessments and
694 ecosystem management in this global hotspot under ongoing and future climate change.
695 More broadly, the HDM-Plot dataset can also contribute to global vegetation ecology
696 by improving the representation of Asian mountain ecosystems in plot-based research.
697 Vegetation plots from southwestern China and the southeastern Tibetan Plateau remain
698 relatively rare in global compilations, despite the high biodiversity and strong
699 environmental heterogeneity of this region. By providing standardized field-based
700 records from this underrepresented mountain system, the dataset can support cross-
701 regional comparisons and large-scale syntheses of vegetation classification,
702 biodiversity patterns, community structure, and ecosystem responses to environmental
703 change.

704 **Author contributions.** JN conceived the study. JN and XM led the field works. YJ, LY,
705 CY, XH, HX, YH, KW, and SS participated in vegetation survey. SS processed the
706 climate maps. YJ and LY processed the dataset, performed the analyses and wrote the
707 first draft. JN, XM and YJ improved the manuscript. All the authors approved the final
708 version of the submitted manuscript.

709 **Competing interests.** The (co-) authors declare that they have no conflict of interest.

710 **Disclaimer.** Publisher's note: Copernicus Publications remains neutral with regard to
711 jurisdictional claims in published maps and institutional affiliations.

712 **Acknowledgements.** The authors sincerely thank Qiuting Chen, Tingting Chen,
713 Zhichao Chen, Tao Fang, Chuting Hu, Saijing Liu, Xiaoling Lu, Chenling Wang,
714 Haoyan Wang, Jie Xia, Yang Yang, Pingqian Ye, Bohan Zheng, Yawen Zheng, and Yan
715 Zhou from Zhejiang Normal University for their help in the field survey, Dashan He
716 from Sichuan University for helping with specimen identification, and Ke Guo from
717 Institute of Botany, the Chinese Academy of Sciences for providing assistance in
718 vegetation classification.

719 **Financial support.** This work was supported by the Second Tibetan Plateau Scientific

720 Expedition and Research Program (grant no. 2019QZKK0402).

721 **References**

722 Chi, X. F., Zhang, F. Q., Gao, Q. B., Xing, R., and Chen, S. L.: Genetic structure and eco-
723 geographical differentiation of *Lancea tibetica* in the Qinghai-Tibetan Plateau, *Genes*, 10, 97,
724 <https://doi.org/10.3390/genes10020097>, 2019.

725 Ding, W. N., Ree, R. H., Spicer, R. A., and Xing, Y. W.: Ancient orogenic and monsoon-driven
726 assembly of the world's richest temperate alpine flora, *Science*, 369, 578–581,
727 <https://doi.org/10.1126/science.abb4484>, 2020.

728 Editorial Committee of the Flora of China: *Reipublicae Popularis Sinicae*, 80 volumes, Science
729 Press, Beijing, 1959–2004.

730 Editorial Committee of Vegetation of China: *Vegetation of China*, Science Press, Beijing, 1980.

731 Editorial Committee of Vegetation Map of China, Chinese Academy of Sciences: *Vegetation of*
732 *China and Its Geographical Pattern – Illustration of the Vegetation Map of the People's*
733 *Republic of China (1:1,000,000)*, Geology Press, Beijing, 2007a.

734 Editorial Committee of Vegetation Map of China, Chinese Academy of Sciences: *Vegetation Map*
735 *of the People's Republic of China (1:1,000,000)*, Geology Press, Beijing, 2007b.

736 Fang, J. Y., Wang, X. P., Shen, Z. H., Tang, Z. Y., He, J. S., Yu, D., Jiang, Y., Wang, Z. H., Zheng,
737 C. Y., Zhu, J. L., and Guo, Z. D.: Methods and protocols for plant community inventory, *Biodiv.*
738 *Sci.*, 17, 533–548, <https://doi.org/10.3724/SP.J.1003.2009.09253>, 2009.

739 Fang, J. Y., Guo, K., Wang, G. H., Tang, Z. Y., Xie, Z. Q., Shen, Z. H., Wang, R. Q., Qiang, S., Liang,
740 C. Z., Da, L. J., and Yu, D.: Vegetation classification system and classification of vegetation
741 types used for the compilation of vegetation of China, *Chin. J. Plant Ecol.*, 44, 96–110, 2020.

742 Farr, T. G., Rosen, P. A., Caro, E., Crippen, R., Duren, R., Hensley, S., Kobrick, M., Paller, M.,
743 Rodriguez, E., Roth, L., Seal, D., Shaffer, S., Shimada, J., Umland, J., Werner, M., Oskin, M.,
744 Burbank, D., and Alsdorf, D.: The Shuttle Radar Topography Mission, *Rev. Geophys.*, 45:
745 RG2004, <https://doi.org/10.1029/2005RG000183>, 2007.

746 Gao, B. C., Fang, W. P., Kong, X. X., Xu, J. M., Guan, Z. T., Yang, J. L., Xiong, J. H., Yi, T. P., Wu,
747 Y. T., Tan, and Z. M.: *Flora of Sichuan*, Sichuan People's Publishing House, Chengdu, 1981.

748 Guo, K., Fang, J. Y., Wang, G. H., Tang, Z. Y., Xie, Z. Q., Shen, Z. H., Wang, R. Q., Qiang, S., Liang,

749 C. Z., Da, L. J., and Yu, D.: A revised scheme of vegetation classification system of China,
750 Chin. J. Plant Ecol., 44, 111–127, <https://doi.org/10.17521/cjpe.2019.0271>, 2020.

751 He, Y. L., Xiong, Q. L., Yu, L., Yan, W. B., and Qu, X. X.: Impact of climate change on potential
752 distribution patterns of alpine vegetation in the Hengduan Mountains region, China, Mt. Res.
753 Dev., 40, R48–R54, <https://doi.org/10.1659/MRD-JOURNAL-D-20-00010.1>, 2020.

754 Hu, X. F., Shi, S. L., Zhou, B. R., and Ni, J.: A 1 km monthly dataset of historical and future climate
755 changes over China. Sci. Data, 12, 436, <https://doi.org/10.1038/s41597-025-04761-y>, 2025.

756 iFlora Initiative of Kunming Institute of Botany, Chinese Academy of Sciences: A Dictionary of the
757 Families and Genera of Chinese Vascular Plants, Science Press, Beijing, 2018.

758 Integrated Scientific Expedition to Qinghai-Tibet Plateau, Chinese Academy of Sciences: Flora
759 Xizangica, 5 volumes, Science Press, Beijing, 1983–1987.

760 Integrated Scientific Expedition to Qinghai-Tibet Plateau, Chinese Academy of Sciences: Physical
761 Geography of Hengduan Mountains, Science Press, Beijing, 1997.

762 Jin, Y. L., Wang, H. Y., Wei, L. F., Hou, Y., Hu, J., Wu, K., Xia, H. J., Xia, J., Zhou, B. R., Li, K.,
763 and Ni, J.: A plot-based dataset of plant community on the Qingzang Plateau, Chin. J. Plant
764 Ecol., 46, 846–854, <https://doi.org/10.17521/cjpe.2022.0174>, 2022.

765 Jin, Y. L., Yang, L. Y. Y., Hu, X. F., Yang, C., Xia, H. J., Hou, Y., Wu, K., Mao, X. X., Ni, J.: A plot-
766 based plant community dataset in the Hengduan Mountains and adjacent regions (2022-2024),
767 Figshare, <https://doi.org/10.6084/m9.figshare.32706207>, 2026a.

768 Jin, Y. L., Yang, L. Y. Y., Hu, X. F., Yang, C., Xia, H. J., Hou, Y., Wu, K., Mao, X. X., Ni, J.: A plot-
769 based plant community dataset in the Hengduan Mountains (2022-2024), National Tibetan
770 Plateau / Third Pole Environment Data Center, <https://doi.org/10.11888/Terre.tpdc.303394>,
771 2026b.

772 Jin, Z. Z.: The Features of Floras in the Dry-hot and Dry-warm Valleys in Yunnan and Sichuan
773 Provinces, Yunnan Science and Technology Press, Kunming, 2002.

774 Jin, Z. Z., and Ou, X. K.: Yuanjiang, Nujiang, Jinshajiang, Lancangjiang Vegetation of Dry Valley,
775 Yunnan University Press & Yunnan Science and Technology Press, Kunming, 2000.

776 Kunming Institute of Botany, Chinese Academy of Sciences: Flora of Yunnan, 21 volumes, Science
777 Press, Beijing, 1977–2006.

778 Li, D. J.: The primary characteristics of flora in the Hengduan Mountainous regions, Mt. Res., 6,

779 147–152, <https://doi.org/10.16089/j.cnki.1008-2786.1988.03.003>, 1988.

780 Li, X. W.: Floristic statistics and analyses of seed plants from China, *Acta Bot. Yunnan.*, 18, 363–
781 384, 1996.

782 Liang, Q. L., Xu, X. T., Mao, K. S., Wang, M. C., Wang, K., Xi, Z. X., and Liu, J. Q.: Shifts in plant
783 distributions in response to climate warming in a biodiversity hotspot, the Hengduan
784 Mountains, *J. Biogeogr.*, 45, 1334–1344, <https://doi.org/10.1111/jbi.13229>, 2018.

785 Liu, Y., Li, P., Xu, Y., Shi, S. L., Ying, L. X., Zhang, W. J., Peng, P. H., and Shen, Z. H.: Quantitative
786 classification and ordination for plant communities in dry valleys of Southwest China, *Biodiv.*
787 *Sci.*, 24, 378–388, <https://doi.org/10.17520/biods.2015241>, 2016a.

788 Liu, Y., Zhu, X. X., Shen, Z. H., and Sun, H.: Flora compositions and spatial differentiations of
789 vegetation in dry valleys of Southwest China, *Biodiv. Sci.*, 24, 367–377,
790 <https://doi.org/10.17520/biods.2015240>, 2016b.

791 Myers, N., Mittermeier, R. A., Mittermeier, C. G., da Fonseca, G. A. B., and Kent, J.: Biodiversity
792 hotspots for conservation priorities, *Nature*, 403, 853–858, <https://doi.org/10.1038/35002501>,
793 2000.

794 Nan, X., Li, A. N., and Deng, W.: Data set of “Digital Mountain Map of China” (2015), National
795 Tibetan Plateau / Third Pole Environment Data Center,
796 <https://doi.org/10.11888/Terre.tpdc.272523>, 2022.

797 Piao, S. L., Zhang, X. Z., Wang, T., Liang, E. Y., Wang, S. P., Zhu, J. T., and Niu, B.: Responses and
798 feedback of the Tibetan Plateau’s alpine ecosystem to climate change, *Chin. Sci. Bull.*, 64,
799 2842–2855, <https://doi.org/10.1360/TB-2019-0074>, 2019.

800 Sabatini, F. M., Lenoir, J., Hattab, T., Arnst, E. A., Chytrý, M., Dengler, J., De Ruffray, P., Hennekens,
801 S. M., Jandt, U., Jansen, F., Jiménez-Alfaro, B., Kattge, J., Levesley, A., Pillar, V. D., Purschke,
802 O., Sandel, B., Sultana, F., Aavik, T., Ačić, S., Acosta, A. T. R., Agrillo, E., Alvarez, M.,
803 Apostolova, I., Arfin Khan, M. A. S., Arroyo, L., Attorre, F., Aubin, I., Banerjee, A., Bauters,
804 M., Bergeron, Y., Bergmeier, E., Biurrun, I., Bjorkman, A. D., Bonari, G., Bondareva, V.,
805 Brunet, J., Čarni, A., Casella, L., Cayuela, L., Černý, T., Chepinoga, V., Csiky, J., Čušterevska,
806 R., De Bie, E., de Gasper, A. L., De Sanctis, M., Dimopoulos, P., Dolezal, J., Dziuba, T., El-
807 Sheikh, M. A. E.-R. M., Enquist, B., Ewald, J., Fazayeli, F., Field, R., Finckh, M., Gachet, S.,
808 Galán-de-Mera, A., Garbolino, E., Gholizadeh, H., Giorgis, M., Golub, V., Alsos, I. G., Grytnes,

809 J.-A., Guerin, G. R., Gutiérrez, A. G., Haider, S., Hatim, M. Z., Hérault, B., Hinojos Mendoza,
810 G., Hölzel, N., Homeier, J., Hubau, W., Indreica, A., Janssen, J. A. M., Jedrzejek, B., Jentsch,
811 A., Jürgens, N., Kaçki, Z., Kapfer, J., Karger, D. N., Kavğacı, A., Kearsley, E., Kessler, M.,
812 Khanina, L., Killeen, T., Korolyuk, A., Kreft, H., Köhl, H. S., Kuzemko, A., Landucci, F.,
813 Lengyel, A., Lens, F., Lingner, D. V., Liu, H., Lysenko, T., Mahecha, M. D., Marcenò, C.,
814 Martynenko, V., Moeslund, J. E., Monteagudo Mendoza, A., Mucina, L., Müller, J. V.,
815 Munzinger, J., Naqinezhad, A., Noroozi, J., Nowak, A., Onyshchenko, V., Overbeck, G. E.,
816 Pärtel, M., Pauchard, A., Peet, R. K., Peñuelas, J., Pérez-Haase, A., Peterka, T., Petřík, P., Peyre,
817 G., Phillips, O. L., Prokhorov, V., Rašomavičius, V., Revermann, R., Rivas-Torres, G., Rodwell,
818 J. S., Ruprecht, E., Rūsiņa, S., Samimi, C., Schmidt, M., Schrod, F., Shan, H., Shirokikh, P.,
819 Šibík, J., Šilc, U., Sklenář, P., Škvorc, Ž., Sparrow, B., Sperandii, M. G., Stančić, Z., Svenning,
820 J.-C., Tang, Z., Tang, C. Q., Tsiripidis, I., Vanselow, K. A., Vásquez Martínez, R., Vassilev, K.,
821 Vélez-Martin, E., Venanzoni, R., Vibrans, A. C., Violle, C., Virtanen, R., von Wehrden, H.,
822 Wagner, V., Walker, D. A., Waller, D. M., Wang, H.-F., Wesche, K., Whitfeld, T. J. S., Willner,
823 W., Wisser, S. K., Wohlgemuth, T., Yamalov, S., Zobel, M., and Bruehlheide, H.: sPlotOpen – An
824 environmentally balanced, open-access, global dataset of vegetation plots, *Glob. Ecol.*
825 *Biogeogr.*, 30, 1740–1764, <https://doi.org/10.1111/geb.13346>, 2021.

826 Shen, Z. H., Liu, Z. L., and Wu, J.: Altitudinal pattern of flora on the eastern slope of Mt. Gongga,
827 *Biodiv. Sci.*, 12, 89–98, <https://doi.org/10.17520/biods.2004011>, 2004.

828 Sherman, R., Mullen, R., Li, H. M., Fang, Z. D., and Wang, Y.: Spatial patterns of plant diversity
829 and communities in alpine ecosystems of the Hengduan Mountains, northwest Yunnan, China,
830 *J. Plant Ecol.*, 1, 117–136, <https://doi.org/10.1093/jpe/rtn012>, 2008.

831 Sloan, S., Jenkins, C. N., Joppa, L. N., Gaveau, D. L. A., and Laurance, W. F.: Remaining natural
832 vegetation in the global biodiversity hotspots, *Biol. Conserv.*, 177, 12–24,
833 <https://doi.org/10.1016/j.biocon.2014.05.027>, 2014.

834 Sun, H., Zhang, J. W., Deng, T., and Boufford, D. E.: Origins and evolution of plant diversity in the
835 Hengduan Mountains, *Plant Divers.*, 39, 161–166, <https://doi.org/10.1016/j.pld.2017.09.004>,
836 2017.

837 Wang, G. H., Fang, J. Y., Guo, K., Xie, Z. Q., Tang, Z. Y., Shen, Z. H., Wang, R. Q., Wang, X. P.,
838 Wang, D. L., Qiang, S., Yu, D., Peng, S. L., Da, L. J., Liu, Q., and Liang, C. Z.: Contents and

839 protocols for the classification and description of vegetation formations, alliances and
840 associations of vegetation of China, *Chin. J. Plant Ecol.*, 44, 128–178,
841 <https://doi.org/10.17521/cjpe.2019.0272>, 2020.

842 Wu, S. H., Pan, T., Cao, J., He, D. M., and Xiao, Z. N.: Barrier-corridor effect of longitudinal range-
843 gorge terrain on monsoons in Southwest China, *Geogr. Res.*, 31, 1–13,
844 <https://doi.org/10.11821/yj2012010001>, 2012.

845 Wu, Z. Y.: The areal-types of Chinese genera of seed plants. *Acta Bot. Yunnan.*, Suppl. IV, 1–139,
846 1991.

847 Wu, Z. Y., Zhou, Z. K., Li, D. Z., Peng, H., and Sun, H.: The areal-types of the world families of
848 seed plants, *Acta Bot. Yunnan.*, 25, 245–257, 2003.

849 Xing, Y. W., and Ree, R. H.: Uplift-driven diversification in the Hengduan Mountains, a temperate
850 biodiversity hotspot, *P. Natl. Acad. Sci. USA*, 114, E3444–E3451,
851 <https://doi.org/10.1073/pnas.1616063114>, 2017.

852 Xu, B., Li, Z. M., and Sun, H.: Plant diversity and floristic characters of the alpine subnival belt
853 flora in the Hengduan Mountains, SW China, *J. Syst. Evol.*, 52, 271–279,
854 <https://doi.org/10.1111/jse.12037>, 2014.

855 Xu, C. D., Feng, J. M., Wang, X. P., and Yang, X.: Vertical distribution patterns of plant species
856 diversity in northern Mt. Gaoligong, Yunnan Province, *Chin. J. Ecol.*, 27, 323–330, 2008.

857 Yang, J. D., Zhang, Z. M., Shen, Z. H., Ou, X. K., Geng, Y. P., and Yang, M. Y.: Review of research
858 on the vegetation and environment of dry-hot valleys in Yunnan, *Biodiv. Sci.*, 24, 462–474,
859 <https://doi.org/10.17520/biods.2015251>, 2016.

860 Yang, Q. Y. and Zheng, D.: An outline of physico-geographic regionalization of the Hengduan
861 Mountains region, *Mt. Res.*, 7, 56–64, <https://doi.org/10.16089/j.cnki.1008-2786.1989.01.010>,
862 1989.

863 Yang, Y., Han, J., Liu, Y., Zhong-Yong, C. R., Shi, S. L., Si-Na, C. L., Xu, Y., Ying, L. X., Zhang,
864 W. J., and Shen, Z. H.: A comparison of the altitudinal patterns in plant species diversity within
865 the dry valleys of the Three Parallel Rivers region, northwestern Yunnan, *Biodiv. Sci.*, 24, 440–
866 452, <https://doi.org/10.17520/biods.2015361>, 2016.

867 Yao, Y. H., Zhang, B. P., Han, F., and Pang, Y.: Diversity and geographical pattern of altitudinal belts
868 in the Hengduan Mountains in China, *J. Mt. Sci.*, 7, 123–132, <https://doi.org/10.1007/s11629->

869 010-1011-9, 2010.

870 Yin, L., Dai, E. F., Zheng, D., Wang, Y. H., Ma, L., and Tong, M.: What drives the vegetation
871 dynamics in the Hengduan Mountain region, southwest China: climate change or human
872 activity?, *Ecol. Indic.*, 112, 106013, <https://doi.org/10.1016/j.ecolind.2019.106013>, 2020.

873 Yu, H. B., Miao, S. Y., Xie, G. W., Guo, X. Y., Chen, Z., and Favre, A.: Contrasting floristic diversity
874 of the Hengduan Mountains, the Himalayas and the Qinghai-Tibet Plateau sensu stricto in
875 China, *Front. Ecol. Evol.*, 8, 136, <https://doi.org/10.3389/fevo.2020.00136>, 2020.

876 Yu, Y. D., Liu, L. H., and Zhang, J. H.: Vegetation regionalization of the Hengduan Mountains region,
877 *Mt. Res.*, 7, 47–55, <https://doi.org/10.16089/j.cnki.1008-2786.1989.01.009>, 1989.

878 Zhang, H. N., Zou, W., Chen, Z., He, L. J., Peng, X. F., Wang, G. Y., Peng, P. H., Li, J. J., and Shi,
879 S. L.: Distribution pattern of plant communities and its relationship with environmental factors
880 in eastern Xizang, China, *Chin. J. Appl. Environ. Biol.*, 29, 1289–1297,
881 <https://doi.org/10.19675/j.cnki.1006-687x.2022.10037>, 2023.

882 Zhang, R. Z., Zheng, D., Yang, Q. Y., and Liu, Y. H.: *Physical Geography of Hengduan Mountains*,
883 Science Press, Beijing, 1997.

884 Zhang, S.R.: *Carex*. In: Hong, D.Y., Sun, H., Watson, M., Wen, J., Zhang, X.C. (eds), *Flora of Pan-*
885 *Himalaya*, Vol. 12, Science Press, Beijing, 2020.

886 Zhang, X. Q., Xu, X. M., Li, X., Cui, P., and Zheng, D.: A new scheme of climate-vegetation
887 regionalization in the Hengduan Mountains region, *Sci. China Earth Sci.*, 67, 751–768,
888 <https://doi.org/10.1007/s11430-023-1231-0>, 2024.

889 Zhang, X. Z., Yang, Y. P., Piao, S. L., Bao, W. K., Wang, S. P., Wang, G. X., Sun, H., Luo, T. X.,
890 Zhang, Y. J., Shi, P. L., Liang, E. Y., Shen, M. G., Wang, J. S., Gao, Q. Z., Zhang, Y. L., and
891 Ouyang, H.: Ecological change on the Tibetan Plateau, *Chin. Sci. Bull.*, 60, 3048–3056,
892 <https://doi.org/10.1360/N972014-01339>, 2015.

893 Zheng, D.: A comparative study on physico-geographic conditions between the Himalayas and
894 Hengduan Mountainous regions, *Mt. Res.*, 6, 137–144, 1988.

895 Zheng, D. and Yang, Q. Y.: Some problems on physico-geographic regionalization of the Hengduan
896 Mountains region, *Mt. Res.*, 5, 7–13, 1987.